Master's Thesis

The Solar Neutrino Day-Night Effect

Mattias Blennow

Mathematical Physics, Department of Physics
Royal Institute of Technology, SE-100 44 Stockholm, Sweden

Stockholm, Sweden 2003

Typeset in LaTeX

Examensarbete inom ämnet fysik för avläggande av civilingenjörsexamen inom utbildningsprogrammet Teknisk Fysik.

Graduation thesis on the subject Physics for the degree of Master of Science in Engineering from the School of Engineering Physics.

TRITA-FYS-2003:51
ISSN 0280-316X
ISRN KTH/FYS/--03:51--SE

Printed in Sweden by Universitetsservice US AB, Stockholm 2003

Abstract

In the standard model of particle physics, neutrinos are necessarily massless. However, recent experiments give strong evidence for neutrino oscillations which can only occur if there are massive neutrinos. Thus, neutrino physics seems to be a way of probing the physics beyond the standard model.

In this thesis, we study the so-called "day-night effect", which concerns solar neutrinos, in a framework of three neutrino flavors. According to the standard solar model, electron neutrinos are produced through thermonuclear reactions in the Sun. However, matter effects in the Sun give rise to a suppression of the electron neutrino flux at the Earth. The day-night effect concerns the influence of the Earth matter effect on the solar electron neutrino survival probability P_S, and thus, the flux of electron neutrinos. In Chapter 1, we briefly review the history of neutrino physics and the standard model of particle physics. Furthermore, we introduce the concept of neutrino oscillations as well as the solar neutrino problem and the day-night effect. In Chapter 2, we assume that there are massive neutrinos and derive expressions for the neutrino oscillation probabilities in vacuum. Chapter 3 is concerned with how the presence of matter affects neutrino oscillations and we also discuss the solar neutrino problem and its solutions. In Chapter 4, we examine the day-night asymmetry in the two flavor framework as well as in the three flavor framework. In particular, we focus on deriving an approximate expression for the electron neutrino survival probability when neutrinos pass through the Earth and discuss the approximations made to derive this expression. Finally, in the last chapter, we summarize and discuss the results obtained in this thesis.

Preface

Neutrino physics is a most interesting field of research in particle physics. Since neutrinos are massless in the standard model of particle physics, neutrino masses and oscillations are probes into the physics beyond the standard model. However, this is not the only reason to be astonished by neutrinos. The mere existence of a particle having a mass, which is several orders of magnitude smaller than the mass of the electron, and in addition, gives so small cross-sections that detectors necessarily need to be huge, is quite interesting in itself.

Considering the properties of neutrinos, it is amazing how much we really do know about them. Despite their small masses, we know that they are massive owing to the observation of neutrino oscillations. These observations further imply mixing in the leptonic sector, where many off-diagonal elements of the mixing matrix are large in contrast to the off-diagonal elements of the mixing matrix in the quark sector. We also know that the presence of matter may significantly alter the neutrino oscillation probabilities through resonant behavior known as the Mikheyev-Smirnov-Wolfenstein effect.

Neutrinos are also of great interest because of the fact that they are produced in many of the thermonuclear reactions, which balance the gravitational forces of stars, and thus, give us a possibility to probe the interior of our own Sun. There are also other aspects of astrophysics, where neutrinos play a significant role. For instance, 99 % of the energy released by a type II supernova is supposed to be carried away by neutrinos and the Big-Bang nucleosynthesis is crucially dependent on the interactions of neutrinos and the number of neutrino flavors.

Quite a few Nobel Prizes have also been awarded for achievements in neutrino physics, the most recent of these being the Prize of 2002, which was awarded jointly to Raymond Davis Jr., Masatoshi Koshiba, and Riccardo Giacconi with 1/4 of the prize each to Davis and Koshiba for "pioneering contributions to astrophysics, in particular for the detection of cosmic neutrinos" and 1/2 of the prize to Giacconi for "pioneering contributions to astrophysics, which have led to the discovery of cosmic X-ray sources".

It has been a pleasure for me to do this master's thesis at the Division of Mathematical Physics, Department of Physics at the Royal Institute of Technology (KTH). I have enjoyed working with elementary particle physics and gaining knowledge in such an interesting field as neutrino physics. I wish to thank everyone who

has made it possible for me to complete this thesis. In particular, I wish to thank my supervisor Håkan Snellman for his support and suggestions and for giving me inspiration. Special thanks are also due to Tommy Ohlsson who has been of great help in giving feedback and suggestions and practically has acted as a second supervisor. I would also like to thank master students Robert Johansson, Tiglet Besara, and Martin Hallnäs, as well as the Ph.D. student Tomas Hällgren for interesting discussions and pleasant lunches, and Walter Winter from Technische Universität München (TUM) for proof reading the last two chapters of this thesis. It was also a pleasure to meet Thomas Schwetz from TUM during the week in September, which he spent at the Division of Mathematical Physics. Thanks are also due to Rickard Armiento and Samuel Rydh for support with computer related issues and also to all others at the Division, in particular, those who have been my lecturers during the past four years. I also wish to thank all of my family, in particular, my parents, who have always been supportive. Last, but not least, I wish to thank my girlfriend Linda Östman for always being my greatest source of inspiration.

Contents

Chapter 1

Introduction to neutrino physics

Since this thesis is concerned with neutrino physics, we will start by giving a short introduction to the subject in this chapter. First of all, we briefly cover the history of neutrino physics. Then, we proceed by reviewing the standard model (SM) of particle physics and discuss why neutrinos are necessarily massless in this model. Finally, we study neutrino oscillations in general and the solar neutrino problem in particular.

1.1 History

In the year 1930, Wolfgang Pauli postulated the existence of a light neutral fermion, which he then called the "neutron" (now known as the "neutrino"), to describe the continuous spectra of the β-decay process

$$ {}^{A}_{Z}X \longrightarrow {}^{A}_{Z+1}Y + e^{-} + \bar{\nu}_e. \tag{1.1} $$

Without the anti-neutrino, the energy of the electron in the β-decay would always be the same (for fixed X). In addition, there would also be non-conservation of angular momentum in the β-decay if the anti-neutrino was not produced. Two years later, Chadwick discovered the particle which is now known as the "neutron" [1]. Chadwick's neutron was obviously not the same particle as Pauli's neutron, since it had a mass of the same order as the proton and Pauli had concluded that his neutron must have a mass of at most one percent of the proton mass. In 1933, Enrico Fermi renamed Pauli's neutron and called it the "neutrino" to distinguish it from the nucleon that we today know as the neutron. The same year, Fermi, Francis, and Perrin [2] came to the conclusion that the neutrino is massless and the year after, Fermi presented his theory of β-decay [3, 4]. Fermi's model of β-decay was the basis for the construction of the Glashow-Weinberg-Salam (GWS)

electroweak model (see Sec. 1.2) and it allowed for the calculation of the cross-sections for reactions in which neutrinos might be detected. The first estimates for the neutrino cross-sections were made by Bethe and Peierls [5].

Since neutrino cross-sections are extremely small, the existence of the neutrino (or rather, the anti-neutrino) was not verified in experiments until the year 1956 [6,7]. On 14 June 1956, Clyde L. Cowan, Jr. and Frederick Reines sent a telegram to Pauli to inform him that they had detected neutrinos through the inverse β-decay

$$\bar{\nu}_e + p \longrightarrow n + e^+. \tag{1.2}$$

Neutrino oscillations were first discussed by Bruno Pontecorvo in 1957 [8, 9] despite the fact that only one neutrino flavor was known at the time. Pontecorvo assumed an analogy between lepton number and strangeness, and in this framework, it is natural to assume that there are $\nu \leftrightarrow \bar{\nu}$ oscillations just as there are $K^0 \leftrightarrow \bar{K}^0$ oscillations. The mixing of two massive neutrinos was first considered in 1962 by Maki, Nakagawa, and Sakata [10] and Nakagawa, *et al.* [11]. In 1967, Pontecorvo applied the idea of neutrino oscillations to the two flavor case of $\nu_e \leftrightarrow \nu_\mu$ oscillations, and two years later, V.N. Gribov and Pontecorvo [12] proposed a phenomenological theory of two flavor neutrino oscillations. Three neutrino flavor mixing was discussed in detail by Samoil M. Bilenky in 1987 [13].

1.2 The standard model of particle physics

The SM is a model describing the fundamental particles and their interactions. It is a very successful theory and it has made a lot of precise predictions. The particle content of the SM is divided into two different types of particles, the quarks, which carry color charge, and the leptons, which do not carry color charge. The quarks and the leptons are further divided into three generations. In the quark sector, the generations are

$$\begin{pmatrix} u \\ d \end{pmatrix}, \begin{pmatrix} c \\ s \end{pmatrix}, \begin{pmatrix} t \\ b \end{pmatrix}, \tag{1.3}$$

where u denotes the up quark, d the down quark, s the strange quark, c the charm quark, b the bottom quark, and t the top quark. In the lepton sector, the generations are

$$\begin{pmatrix} e \\ \nu_e \end{pmatrix}, \begin{pmatrix} \mu \\ \nu_\mu \end{pmatrix}, \begin{pmatrix} \tau \\ \nu_\tau \end{pmatrix}, \tag{1.4}$$

where e denotes the electron, μ the muon, τ the tauon, and ν_x ($x = e, \mu, \tau$) denotes the corresponding neutrino. The SM also includes the anti-particles of the above mentioned particles. The quarks carry an electric charge of $+\frac{2}{3}$ (u, c, t) or $-\frac{1}{3}$ (d, s, b), while the charged leptons (e, μ, τ) carry the electric charge of -1 and the neutrinos do not carry any electric charge. The SM also contains twelve gauge bosons, which are the carriers of the electromagnetic (the photon), weak ($W^\pm$ and Z^0), and strong (eight gluons) interactions, respectively, as well as the Higgs field

responsible for yielding an effective mass term for the carriers of the weak interaction as well as the massive particles. Since this thesis is concerned with neutrinos, we concentrate on the leptonic sector of the SM in which only the electroweak interactions are present.

1.2.1 The electroweak model

The model for the electroweak interaction is known as the Glashow-Weinberg-Salam (GWS) electroweak model [14–16] and it is based on the symmetry group $SU(2)_L \otimes U(1)_Y$. Let us denote the gauge fields by $W^{i,\mu}$ (for $SU(2)_L$) and B^μ (for $U(1)_Y$), and use only one generation of leptons for simplicity. Using the notation

$$L = \begin{pmatrix} \nu_{\ell L} \\ \ell_L \end{pmatrix}, \quad R = \ell_R, \tag{1.5}$$

the Lagrangian density is given by

$$\mathcal{L}_0 = -\frac{1}{4}\mathcal{F}^{\mu\nu}\mathcal{F}_{\mu\nu} - \frac{1}{4}\mathcal{W}^{\mu\nu}\mathcal{W}_{\mu\nu} + \mathrm{i}\bar{L}\gamma^\mu D_\mu L + \mathrm{i}\bar{R}\gamma^\mu D_\mu R, \tag{1.6}$$

where

$$\mathcal{F}^{\mu\nu} = \partial^\mu B^\nu - \partial^\nu B^\mu, \quad \mathcal{W}^{\mu\nu} = \partial^\mu \boldsymbol{W}^\nu - \partial^\nu \boldsymbol{W}^\mu + g\boldsymbol{W}^\mu \times \boldsymbol{W}^\nu \tag{1.7}$$

are the gauge field strengths, $\boldsymbol{W}^\mu = \begin{pmatrix} W^{1,\mu} & W^{2,\mu} & W^{3,\mu} \end{pmatrix}^T$, $D_\mu = \partial_\mu - \mathrm{i}g'\frac{Y}{2}B_\mu - \mathrm{i}g\frac{\boldsymbol{\tau}}{2}\cdot\boldsymbol{W}_\mu$ is the covariant derivative, g and g' are coupling constants, Y is the weak hypercharge operator, and $\boldsymbol{\tau}$ is a vector of Pauli matrices. Note that only the left-handed neutrino fields are present in the SM. The interaction part of the Lagrangian density becomes

$$\begin{aligned} \mathcal{L}_{0,\mathrm{int}} &= \frac{g}{\sqrt{2}}(j^{+\mu}W_\mu + j^{-\mu}W_\mu^\dagger) + (g\cos\theta_W j^{3\mu} - g'\sin\theta_W j^{\frac{Y}{2}\mu})Z_\mu \\ &\quad + (g\sin\theta_W j^{3\mu} + g'\cos\theta_W j^{\frac{Y}{2}\mu})A_\mu, \end{aligned} \tag{1.8}$$

where we have introduced the currents

$$j^{\frac{Y}{2}\mu} = \bar{L}\gamma^\mu\frac{Y}{2}L + \bar{R}\gamma^\mu\frac{Y}{2}R, \tag{1.9}$$

$$j^{a\mu} = \bar{L}\gamma^\mu\frac{\tau^a}{2}L, \tag{1.10}$$

and the fields

$$W_\mu = \frac{W_\mu^1 - \mathrm{i}W_\mu^2}{\sqrt{2}}, \quad W_\mu^\dagger = \frac{W_\mu^1 + \mathrm{i}W_\mu^2}{\sqrt{2}},$$

$$Z_\mu = \cos\theta_W W_\mu^3 - \sin\theta_W B_\mu, \quad A_\mu = \sin\theta_W W_\mu^3 + \cos\theta_W B_\mu. \tag{1.11}$$

Here θ_W is the so-called Weinberg angle. In Eq. (1.8), the last term is to be identified with the standard electromagnetic interaction $\mathcal{L}_{\mathrm{EM}} = ej^\mu_{\mathrm{EM}}A_\mu$, and thus,

$ej^{\mu}_{\rm EM} = g\sin\theta_W j^{3\mu} + g'\cos\theta_W j^{\frac{Y}{2}\mu}$. For the weak analogue of the Gell-Mann-Nishijima relation [17, 18]

$$Q = I_3 + \frac{Y}{2}, \tag{1.12}$$

where I_3 is the third component of the isospin, to hold, we obtain the condition

$$j^{\mu}_{\rm EM} = j^{3\mu} + j^{\frac{Y}{2}\mu} \tag{1.13}$$

for the currents. It follows that $e = g\sin\theta_W = g'\cos\theta_W$ and the weak interaction part of the Lagrangian density becomes

$$\mathcal{L}^{\rm weak}_{0,\rm int} = \frac{g}{\sqrt{2}}(j^{+\mu}W_\mu + j^{-\mu}W^\dagger_\mu) + \frac{g}{2\cos\theta_W} j^{Z\mu}Z_\mu, \tag{1.14}$$

where the currents are explicitly given by

$$j^{+\mu} = \bar{\nu}_{\ell L}\gamma^\mu \ell_L, \tag{1.15}$$
$$j^{-\mu} = \bar{\ell}_L\gamma^\mu \nu_{\ell L}, \tag{1.16}$$
$$j^{Z\mu} = \bar{\nu}_{\ell L}\gamma^\mu \nu_{\ell L} - \bar{\ell}_L\gamma^\mu \ell_L + 2\sin^2\theta_W \bar{\ell}\gamma^\mu \ell. \tag{1.17}$$

The $SU(2)_L \otimes U(1)_Y$ gauge symmetry requires that the masses of all fields are set to zero. The GWS electroweak theory is based on a spontaneous breaking of this gauge symmetry to the $U(1)_{\rm EM}$ symmetry of electromagnetic interactions. This spontaneous symmetry breaking is implemented by the Higgs mechanism [19–22]. Let us introduce a complex doublet Higgs field $\Phi = \begin{pmatrix} \phi^+ & \phi^0 \end{pmatrix}^T$ with hypercharge $Y = 1$ as well as the Higgs Lagrangian density

$$\mathcal{L}_{\rm Higgs} = (D^\mu\Phi)^\dagger(D_\mu\Phi) + \mu^2\Phi^\dagger\Phi - \lambda(\Phi^\dagger\Phi)^2. \tag{1.18}$$

This gives a vacuum expectation value[1]

$$\langle\Phi\rangle_0 = \begin{pmatrix} 0 \\ \frac{v}{\sqrt{2}} \end{pmatrix}, \tag{1.19}$$

where $v = \sqrt{\frac{\mu^2}{2\lambda}}$. This vacuum expectation value gives us the effective masses

$$m_W = \frac{gv}{2}, \quad m_Z = \frac{gv}{2\cos\theta_W}, \quad m_A = m_\gamma = 0, \tag{1.20}$$

where m_γ is the effective photon mass. In order to obtain the charged lepton masses, we introduce the Yukawa coupling term

$$\mathcal{L}_{\rm Yuk} = -G_\ell(\bar{L}\Phi R + \bar{R}\Phi^\dagger L), \tag{1.21}$$

[1] There is some freedom in choosing the vacuum state, we choose it such that Eq. (1.19) is fulfilled.

where G_ℓ is a dimensionless coupling constant known as the Yukawa coupling, in the Lagrangian density. This yields an effective charged lepton mass of

$$m_\ell = \frac{G_\ell v}{\sqrt{2}}. \tag{1.22}$$

At first sight, one might think of using an approach similar to the one used to introduce charged lepton masses to introduce neutrino masses into the SM. However, this is not possible, since there are no right-handed neutrino fields in the SM. One might then think that effective neutrino masses could arise from higher order loop corrections. However, this is not the case, since such effective masses would break the accidental SM symmetry $B - L$ [23]. Thus, if there are neutrino masses, the SM is not a complete description of Nature and some new physics is needed to incorporate neutrino masses into a model of particle physics. The introduction of neutrino masses can be done in a number of ways, all demanding the existence of a right-handed neutrino field.

1.3 Neutrino oscillations

Basically, the concept of neutrino oscillations is based on neutrinos being produced in one flavor state and detected in another flavor state. If a neutrino is produced as an electron neutrino ν_e and detected as a muon neutrino ν_μ, one speaks about $\nu_e \leftrightarrow \nu_\mu$ oscillations.

As will be shown in Chapter 2, neutrino oscillations can only occur if there are massive neutrinos. In addition, for neutrino oscillations to occur, the neutrino mass eigenstates $|\nu_i\rangle$ (the neutrino states with definite mass) must not be the same as the neutrino flavor eigenstates $|\nu_\alpha\rangle$ (the neutrino states participating in the weak interactions with the charged leptons). This is known as mixing of neutrinos. In the extreme relativistic limit, the neutrino oscillations do not depend on the absolute mass scale, but rather on the mass squared differences $\Delta m^2_{ij} = m^2_i - m^2_j$, where m_i is the mass of the neutrino mass eigenstate $|\nu_i\rangle$.

Neutrino oscillations may be detected by appearance or disappearance of neutrinos of some given flavor in neutrino fluxes with known initial composition. For example, electron anti-neutrinos $\bar{\nu}_e$ are produced in nuclear reactors giving an initial flow of $\bar{\nu}_e$ only. Oscillations in this case may be measured by a deficit in the observed number of events in a detector compared with the predicted number of events. As another example, electron neutrinos ν_e and muon neutrinos ν_μ are produced when cosmic rays hit the Earth's atmosphere. Oscillations of neutrinos can be detected by comparing the ratios of the ν_e and ν_μ fluxes when neutrinos are detected before (neutrinos entering the detector from above) and after (neutrinos entering the detector from below) passing through the Earth.

As we will discuss in Chapter 3, neutrino oscillations may be significantly altered in the presence of matter and even in the case of small mixing, there may be

large oscillation probabilities due to resonant oscillations known as the Mikheyev-Smirnov-Wolfenstein (MSW) effect.

1.4 Solar neutrinos and day-night effect

The standard solar model (SSM) [24] predicts a flux of electron neutrinos ν_e that is produced in the Sun through thermonuclear reactions. However, neutrino detectors observe that there is a deficit in the experimentally measured ν_e flux compared with the predicted flux. This deficit, known as the "solar neutrino problem", may be interpreted as a flaw in the SSM. However, the SSM agrees remarkably well with other experimental data and the remaining conclusion is that either the calculations of solar neutrino cross-sections are incorrect or that there really is a disappearance of solar electron neutrinos on their way from the Sun to the Earth. As in the case of the SSM, there are reasons to believe that the calculated cross-sections for the solar neutrinos are fairly accurate and the remaining solution is the disappearance of electron neutrinos. This is supported by the experimental data from the Sudbury Neutrino Observatory neutral-current measurements and the most plausible description of the deficit in the solar electron neutrino flux as compared with the prediction of the SSM is oscillations of electron neutrinos ν_e into the other neutrino flavors ν_μ and ν_τ. The solar neutrino problem will be discussed in more detail in Sec. 3.5.

As was mentioned in the previous section, the presence of matter may influence neutrino oscillations in a significant way. A legitimate question is therefore if the survival probability of solar electron neutrinos being detected as electron neutrinos is affected by passing through the Earth. The answer is that there might well be such an effect and that the magnitude of this effect is dependent on the fundamental neutrino oscillation parameters (the masses and the mixing of neutrinos) as well as the neutrino energy. This effect is known as the day-night effect, since neutrinos pass through the Earth before detection in nighttime, but not in daytime.

Chapter 2

Neutrino oscillations

2.1 Neutrino masses

In the SM, neutrinos are massless particles. However, there is now strong evidence for neutrino oscillations [25–34], which, as we will see, can only occur if there are massive neutrinos.

In the case of a Dirac neutrino mass term, the part of the Lagrangian density $\mathcal{L}_\ell$, describing the masses and weak interactions of charged leptons and neutrinos, is given by [35]

$$\mathcal{L}_\ell = -\frac{g}{\sqrt{2}}\bar{\ell}_{\alpha L}\gamma^\mu \nu_{\alpha L} W_\mu^\dagger - \bar{\ell}_{\alpha L}(M_\ell)_{\alpha\beta}\ell_{\beta R} - \bar{\nu}_{\alpha L}(M_\nu)_{\alpha\beta}\nu_{\beta R} + \text{h.c.}, \tag{2.1}$$

where g is a coupling constant, ℓ_α denotes the charged lepton flavor eigenfields, ν_α the neutrino flavor eigenfields, W is one of the weak gauge fields, M_ℓ the charged lepton mass matrix, and M_ν the neutrino mass matrix. We define the lepton mass eigenfields (we will use Latin indices for mass eigenfields and Greek indices for flavor eigenfields) by

$$\nu_{iL} = (U_L^\dagger)_{i\alpha}\nu_{\alpha L},\ \nu_{iR} = (U_R^\dagger)_{i\alpha}\nu_{\alpha R},\ \ell_{iL} = (V_L^\dagger)_{i\alpha}\ell_{\alpha L},\ \ell_{iR} = (V_R^\dagger)_{i\alpha}\ell_{\alpha R}, \tag{2.2}$$

where U_C and V_C ($C \in \{L, R\}$) are unitary transformations such that

$$U_L^\dagger M_\nu U_R = \mathcal{M}_\nu, \quad V_L^\dagger M_\ell V_R = \mathcal{M}_\ell, \tag{2.3}$$

where $\mathcal{M}_\nu$ and $\mathcal{M}_\ell$ are diagonal matrices. The charged lepton flavor eigenstates may be defined in such a way that V_C is diagonal and only contain phases.

Now, the Lagrangian density $\mathcal{L}_\ell$ can be expressed as

$$\mathcal{L}_\ell = -\frac{g}{\sqrt{2}}\bar{\ell}_{iL}\gamma^\mu U_{ij}\nu_{jL}W_\mu^\dagger - \bar{\ell}_{iL}(\mathcal{M}_\ell)_{ij}\ell_{jR} - \bar{\nu}_{iL}(\mathcal{M}_\nu)_{ij}\nu_{jR} + \text{h.c.}, \tag{2.4}$$

where $U = V_L^\dagger U_L$ is the so-called leptonic mixing matrix[1]. In general, an n-dimensional unitary matrix can be parameterized by n^2 real parameters, $n(n-1)/2$ Euler angles, and $n(n+1)/2$ phases. However, for Dirac fields, we may absorb some phases into the fields without changing the physics. It follows that for n generations of Dirac neutrinos, we may absorb phases by redefining the phases of the n charged lepton fields and the n neutrino fields. Suppose that we change the phases of the fields so that $\ell_i \to e^{\mathrm{i}\varphi_i}\ell_i$ and $\nu_i \to e^{\mathrm{i}\psi_i}\nu_i$, the new mixing matrix is then given by

$$U' = e^{\mathrm{i}(\varphi_1-\psi_1)}\Psi_\ell U \Psi_\nu^\dagger, \tag{2.5}$$

where $\Psi_\ell = \mathrm{diag}(1, e^{\mathrm{i}(\varphi_2-\varphi_1)}, e^{\mathrm{i}(\varphi_3-\varphi_1)}, \ldots)$, $\Psi_\nu = \mathrm{diag}(1, e^{\mathrm{i}(\psi_2-\psi_1)}, e^{\mathrm{i}(\psi_3-\psi_1)}, \ldots)$, and U is the original leptonic mixing matrix. Thus, it is clear that we may absorb one overall phase $(\varphi_1 - \psi_1)$, $n-1$ phases into the charged lepton fields $(\varphi_i - \varphi_1)$, and $n-1$ phases into the neutrino fields $(\psi_i - \psi_1)$. This leaves $(n-1)(n-2)/2$ physical phases.

In the case of a Majorana mass term, the situation is similar to that of Dirac neutrinos. However, the phases of Majorana fields cannot be redefined, and thus, only n phases of the mixing matrix may be eliminated (through the redefinition of the charged lepton fields) leaving $n(n-1)/2$ physical phases in the case of Majorana neutrinos.

2.2 The Schrödinger equation for neutrino propagation

The Dirac equation for the propagation of a neutrino mass eigenfield ν is given by

$$(\mathrm{i}\gamma^\mu\partial_\mu - m\mathbf{1})\nu = 0, \tag{2.6}$$

where $\mathbf{1}$ is the 4×4 identity matrix and m the neutrino mass. Multiplying by $\mathrm{i}\gamma^\mu\partial_\mu + m\mathbf{1}$ from the left, one obtains the Klein-Gordon equation

$$(\partial^\mu\partial_\mu + m^2)\nu = 0. \tag{2.7}$$

The Klein-Gordon equation does not reveal the spin structure of the neutrino, but since neutrino masses are small, we will be dealing with ultra-relativistic neutrinos

[1] Also known as the Maki-Nakagawa-Sakata (MNS) matrix [36], which is the lepton sector equivalent of the Cabibbo-Kobayashi-Maskawa (CKM) matrix [37, 38] in the quark sector.

for which the spin structure is not revealed anyway. Using the substitutions $\mathrm{i}\frac{\partial}{\partial t} \to E$ and $-\mathrm{i}\frac{\partial}{\partial \boldsymbol{x}} \to \boldsymbol{p}$, we obtain

$$(\boldsymbol{p}^2 + m^2)\nu = E^2\nu \tag{2.8}$$

and the familiar relativistic formula $E^2 = \boldsymbol{p}^2 + m^2$ is clearly fulfilled for the mass eigenfield. It follows that also $E = \sqrt{\boldsymbol{p}^2 + m^2}$. Assuming that $|\boldsymbol{p}| \gg m$, which is equivalent to assuming a relativistic neutrino, we obtain

$$E \simeq p + \frac{m^2}{2p}, \tag{2.9}$$

where $p = |\boldsymbol{p}|$. We now make the substitution $E \to \mathrm{i}\frac{\partial}{\partial t}$ and obtain the Schrödinger equation for neutrino propagation as

$$\mathrm{i}\frac{\partial \nu}{\partial t} = \left(p + \frac{m^2}{2p}\right)\nu = H\nu, \tag{2.10}$$

with the plane-wave solution

$$\nu(\boldsymbol{x}, t) = \exp\left(-\mathrm{i}\left(p + \frac{m^2}{2p}\right)t\right)\nu(\boldsymbol{x}, 0). \tag{2.11}$$

If we have n neutrino mass eigenfields with momentum p, then the time evolution is given by Eq. (2.10), where $\nu = \begin{pmatrix} \nu_1 & \nu_2 & \dots & \nu_n \end{pmatrix}^T$ and m is a diagonal matrix, whose elements are the masses of the neutrino mass eigenfields.

2.3 Neutrino oscillations with n flavors

If the neutrino mixing is given by

$$\nu_{\alpha L} = U_{\alpha i}\nu_{iL}, \tag{2.12}$$

then the state vector of a neutrino flavor eigenstate becomes [39]

$$|\nu_\alpha\rangle = U^*_{\alpha i}\,|\nu_i\rangle\,. \tag{2.13}$$

Now, suppose that we have a complete set of neutrino states $S = \{|k\rangle\}$, we then use the somewhat sloppy notation $|\nu\rangle_S$ to denote the representation of the neutrino state $|\nu\rangle$ in the S-basis, i.e.,

$$|\nu\rangle_S = \begin{pmatrix} \langle 1|\nu\rangle \\ \langle 2|\nu\rangle \\ \vdots \\ \langle n|\nu\rangle \end{pmatrix} \equiv \begin{pmatrix} \phi_1^S \\ \phi_2^S \\ \vdots \\ \phi_n^S \end{pmatrix}. \tag{2.14}$$

For the particular case of flavor and mass eigenstate bases, we will use the notation ϕ_α and ϕ_i for the components of the neutrino state with the definitions

$$\phi_\alpha = \langle \nu_\alpha | \nu \rangle \,, \quad \phi_i = \langle \nu_i | \nu \rangle \,. \tag{2.15}$$

From Eq. (2.13) it follows that

$$\phi_\alpha = \langle \nu_\alpha | \nu \rangle = U_{\alpha i} \langle \nu_i | \nu \rangle = U_{\alpha i} \phi_i, \tag{2.16}$$

and thus, we have

$$|\nu\rangle_f = U \, |\nu\rangle_m \,, \tag{2.17}$$

where f and m denote the flavor and mass eigenstate bases, respectively. The time evolution of the neutrino state $|\nu\rangle$ will be on the form

$$\mathrm{i} \frac{\mathrm{d} \, |\nu\rangle_S}{\mathrm{d}t} = H_S \, |\nu\rangle_S \,. \tag{2.18}$$

From Eq. (2.11) it follows that

$$H_m = p\mathbf{1} + \frac{1}{2p} \begin{pmatrix} m_1^2 & 0 & \dots & 0 \\ 0 & m_2^2 & \dots & 0 \\ \vdots & \vdots & \ddots & \vdots \\ 0 & 0 & \dots & m_n^2 \end{pmatrix} \tag{2.19}$$

and due to the relation in Eq. (2.17), we have

$$H_f = U H_m U^\dagger. \tag{2.20}$$

Suppose that a neutrino is produced in the flavor eigenstate $|\nu_\alpha\rangle$ with a well-defined momentum p. If we denote the neutrino state at time t by $|\nu(t)\rangle$, then the solution to Eq. (2.18) in mass basis is given by

$$\phi_i(t) \simeq e^{-\mathrm{i}\frac{m_i^2}{2p}t} \phi_i(0) = e^{-\mathrm{i}\frac{m_i^2}{2p}t} \langle \nu_i | \nu_\alpha \rangle = e^{-\mathrm{i}\frac{m_i^2}{2p}t} U_{\alpha i}^*, \tag{2.21}$$

where we have dropped the phase $e^{-\mathrm{i}pt}$, which is common for all components. The oscillation probability $P_{\alpha\beta}(t)$ of finding the neutrino in the flavor eigenstate $|\nu_\beta\rangle$ at time t is then obtained as

$$\begin{aligned} P_{\alpha\beta}(t) &= |\, \langle \nu_\beta | \nu(t) \rangle \,|^2 \\ &= |\sum_{i=1}^{n} \langle \nu_\beta | \nu_i \rangle \, \langle \nu_i | \nu(t) \rangle \,|^2 \\ &= \left| \sum_{i=1}^{n} e^{-\mathrm{i}\frac{m_i^2}{2p}t} U_{\beta i} U_{\alpha i}^* \right|^2 \\ &= \sum_{i=1}^{n} \sum_{j=1}^{n} U_{\alpha i}^* U_{\beta i} U_{\alpha j} U_{\beta j}^* e^{\mathrm{i}\frac{\Delta m_{ji}^2}{2E}t}, \end{aligned} \tag{2.22}$$

where $\Delta m^2_{ij} = m^2_i - m^2_j$. For $t = 0$, unitarity yields $P_{\alpha\beta}(0) = \delta_{\alpha\beta}$. The oscillation probabilities depend only on the entries of the leptonic mixing matrix U, the difference of the neutrino masses squared Δm^2_{ij}, and the time t. If the mixing matrix is real, then $U^*_{\alpha i} = U_{\alpha i}$ and $P_{\alpha\beta}(t) = P_{\beta\alpha}(t)$, i.e., we have T-invariance. Assuming CPT-invariance, this also induces CP-invariance, i.e., the same probabilities for neutrinos as for anti-neutrinos. Thus, when CP is conserved, then the mixing matrix is real.

2.4 Two flavor neutrino oscillations

According to our previous discussion, for Dirac neutrinos, the leptonic mixing matrix U may be taken to be real, i.e., orthogonal, in the two flavor case. The standard parameterization used for the 2×2 mixing matrix is

$$U = \begin{pmatrix} c & s \\ -s & c \end{pmatrix}, \tag{2.23}$$

where $s = \sin\theta$, $c = \cos\theta$, and the angle θ, known as the "mixing angle", is a fundamental parameter of the neutrino theory.

Suppose that the two neutrino flavors are ν_e and ν_x. Using the parameterization of Eq. (2.23), the two flavor oscillation probabilities are given by

$$P_{ex}(t) = P_{xe}(t) = \sin^2(2\theta)\sin^2\left(\frac{\Delta m^2}{4E}t\right), \tag{2.24}$$

where $\Delta m^2 = m^2_2 - m^2_1$, and we have used that for relativistic neutrinos $p \simeq E$. We should not be surprised by the fact that $P_{ex}(t) = P_{xe}(t)$, since, in the two flavor case, the mixing matrix is real. For relativistic neutrinos, we also have the relation $t \simeq L$, where L is the distance traveled by the neutrinos, and thus, we may write the oscillation probabilities as a function of the traveled distance

$$P_{ex}(L) = \sin^2(2\theta)\sin^2\left(\frac{\Delta m^2}{4E}L\right). \tag{2.25}$$

From the unitarity conditions $P_{e\beta} + P_{x\beta} = P_{\alpha e} + P_{\alpha x} = 1$, where $\alpha, \beta \in \{e, x\}$ we deduce that $P_{ee}(L) = P_{xx}(L) = 1 - P_{ex}(L)$.

In Eq. (2.25), the $\sin^2(2\theta)$ factor is constant and represents the amplitude of the oscillations. We also define the oscillation length $L_{\rm osc}$ as

$$L_{\rm osc} = \frac{4\pi E}{\Delta m^2}, \tag{2.26}$$

which is the length needed to complete one period of oscillation.

One might ask how good the approximation $\sqrt{p^2+m^2} \simeq p + \frac{m^2}{2p}$ really is. If we include one more term of the series expansion, then we obtain

$$\sqrt{p^2+m^2} \simeq p\left(1+\frac{m^2}{2p^2}+\frac{m^4}{4p^4}\right). \tag{2.27}$$

Suppose we have two flavor neutrino oscillations and the masses of the mass eigenstates are given by m_1 and m_2, respectively. Then the difference between the energies, E_1 and E_2, respectively, of the mass eigenstates is given by

$$\begin{aligned} E_2 - E_1 &\simeq p\left(1+\frac{m_2^2}{2p^2}+\frac{m_2^4}{4p^4}\right) - p\left(1+\frac{m_1^2}{2p^2}+\frac{m_1^4}{4p^4}\right) \\ &= \frac{\Delta m^2}{2p}\left(1-\frac{m_2^2+m_1^2}{2p^2}\right), \end{aligned} \tag{2.28}$$

and thus, the relative correction given by including one more term of the series expansion is $\frac{m_2^2+m_1^2}{2p^2}$. If we have $m_2 \gg m_1$ and a mass squared difference of $\Delta m^2 \simeq 10^{-2}$ eV^2, which is larger than the value for the atmospheric mass squared difference, and further assume that the neutrinos we detect will have energies larger than 1 MeV, then the relative correction is of the order 10^{-14}. This corresponds to the relative correction in the oscillation length $L_{\rm osc}$ and this correction is, at present, far from measurable.

2.5 Three flavor neutrino oscillations

In the case of three neutrino flavors (ν_e, ν_μ, and ν_τ), the leptonic mixing matrix U can be parameterized by three Euler angles and one phase. The standard parameterization is given by [40]

$$U = \begin{pmatrix} c_{13}c_{12} & c_{13}s_{12} & s_{13}e^{-\mathrm{i}\delta} \\ -s_{12}c_{23} - c_{12}s_{23}s_{13}e^{\mathrm{i}\delta} & c_{12}c_{23} - s_{12}s_{23}s_{13}e^{\mathrm{i}\delta} & s_{23}c_{13} \\ s_{12}s_{23} - c_{12}c_{23}s_{13}e^{\mathrm{i}\delta} & -c_{12}s_{23} - s_{12}c_{23}s_{13}e^{\mathrm{i}\delta} & c_{23}c_{13} \end{pmatrix}, \tag{2.29}$$

where $s_{ij} = \sin\theta_{ij}$, $c_{ij} = \cos\theta_{ij}$, δ is the CP-violating phase, and θ_{ij} are the leptonic mixing angles. We also assume that there is a mass squared difference hierarchy such that

$$|\Delta m^2_{21}| \ll |\Delta m^2_{31}| \simeq |\Delta m^2_{32}|, \tag{2.30}$$

which is indicated by the solar and atmospheric neutrino experiments [25, 28, 29, 31–34].

In general, the case of three flavor neutrino oscillations does not lead to probabilities of a form as simple as that in the two flavor case. However, there are a number of limiting cases in which the three flavor neutrino oscillation effectively

turns into an oscillation between two flavors, for example, in the limit of $\Delta m^2_{21} \to 0$, we have

$$P_{\alpha\beta}(L) \longrightarrow 4|U_{\alpha 3}|^2|U_{\beta 3}|^2 \sin^2\left(\frac{\Delta m^2_{31}}{4E}L\right). \tag{2.31}$$

As another example, we may consider when $|\Delta m^2_{31}| \simeq |\Delta m^2_{32}| \gg 2E/L$. In this case, oscillations due to Δm^2_{31} and Δm^2_{32} are fast and give an averaged effect, the resulting survival probability for ν_e is then given by

$$P_{ee}(L) \simeq c^4_{13}P + s^4_{13}, \tag{2.32}$$

where P is the ν_e survival probability in the two flavor case with $\theta = \theta_{12}$ and $\Delta m^2 = \Delta m^2_{21}$.

2.6 Majorana neutrino oscillations

As was briefly mentioned in the beginning of this chapter, in the case of Majorana neutrinos, there is a possibility of having more phases in the leptonic mixing matrix. The general leptonic mixing matrix in the case of Majorana neutrinos can be parameterized by

$$U = U^{\mathrm{D}}D, \tag{2.33}$$

where U^{D} is the leptonic mixing matrix in the case of Dirac neutrinos, and D is a diagonal unitary matrix (the elements on the diagonal are the Majorana phases).

We now ask the question: "Are the Majorana phases observable in neutrino oscillations?" The answer to this question is "no". The reason is that in the oscillation formula Eq. (2.22), we have

$$U_{\beta i}U^*_{\alpha i} = U^{\mathrm{D}}_{\beta j}D_{ji}D^*_{ki}U^{\mathrm{D}*}_{\alpha k} = e^{\mathrm{i}(\varphi_i-\varphi_i)}U^{\mathrm{D}}_{\beta i}U^{\mathrm{D}*}_{\alpha i} = U^{\mathrm{D}}_{\beta i}U^{\mathrm{D}*}_{\alpha i}, \tag{2.34}$$

where $e^{\mathrm{i}\varphi_i}$ is the ith element on the diagonal, and there is no summation over the index i. It follows that the oscillation probabilities do not depend on the Majorana phases, and thus, these are not observable in neutrino oscillations.

Chapter 3

Neutrinos in matter

In this chapter, we will discuss why and how neutrino oscillations are affected when matter is present. We will assume the matter to be "ordinary" in the sense that it is mainly composed of electrons, protons, and neutrons. We will also assume that one of the neutrino flavors involved in the oscillations is the electron neutrino ν_e. As we will see, there can be quite significant changes to the oscillation probabilities when neutrinos propagate through matter [41,42]. For example, in the two flavor case, the probability of a flavor change is at most $\sin^2\theta$. However, when neutrinos propagate through matter, the Mikheyev-Smirnov-Wolfenstein (MSW) effect can lead to large oscillation probabilities even in the case of a very small leptonic mixing angle θ.

3.1 Matter propagation with n neutrino flavors

Neutrinos which propagate in matter may be affected in a number of ways by interactions with the matter constituents, the neutrinos may be absorbed or scattered. In general, these processes have small probabilities which, to leading order, are proportional to the Fermi coupling constant G_F squared. There is also the effect of coherent forward-scattering of neutrinos, which leads to an effective potential V_α for the neutrino flavors. This potential is proportional to G_F and one might expect the effects to be negligible. However, the energy difference between different neutrino mass eigenstates is also small and, if the differences in V_α for different flavors should be comparable to or larger than $\frac{\Delta m^2}{2E}$, then the oscillations can be significantly affected by matter effects.

Let us consider the case of n neutrino flavors where one of the flavors is the electron neutrino ν_e. There are two types of weak interactions, the charged-current (CC) interaction, which is mediated by the exchange of $W^\pm$ gauge bosons, and the neutral-current (NC) interaction, which is mediated by the exchange of Z^0 gauge bosons. For forward-scattering, only the electron neutrinos are affected by the CC

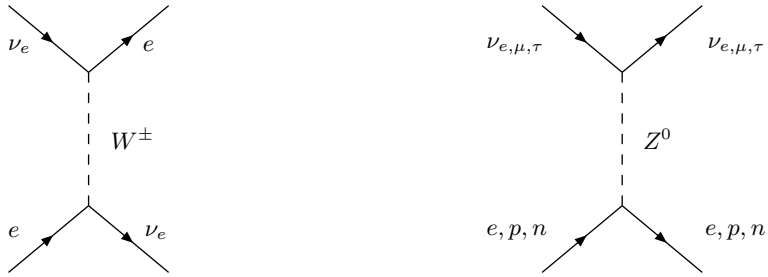

Figure 3.1. Feynman diagrams for CC and NC forward-scattering in matter.

interactions, while the NC interactions occur for all neutrino flavors. The Feynman diagrams for CC and NC forward-scattering in matter are shown in Fig. 3.1.

At low energies, the effective CC Hamiltonian is given by [43]

$$H_{CC} = \frac{G_F}{\sqrt{2}}[\bar{e}\gamma^{\mu}(1-\gamma_5)\nu_e][\bar{\nu}_e\gamma_{\mu}(1-\gamma_5)e], \tag{3.1}$$

which can be rewritten as

$$H_{CC} = \frac{G_F}{\sqrt{2}}[\bar{e}\gamma_{\mu}(1-\gamma_5)e][\bar{\nu}_e\gamma^{\mu}(1-\gamma_5)\nu_e] \tag{3.2}$$

by using the Fierz transformation. In order to obtain the effective CC potential for the electron neutrino, we integrate H_{CC} over the variables belonging to the electron fields. The coherent forward-scattering is implemented by assuming the same momentum for the incoming and scattered electron. Assuming a non-polarized medium with zero average momentum, one obtains

$$H_{CC,\text{eff}} = V_{CC}\bar{\nu}_e\nu_e, \tag{3.3}$$

where $V_{CC} = \sqrt{2}G_F N_e$, G_F is the Fermi coupling constant and N_e the electron number density. In the same manner, one obtains the NC effective potential as

$$H_{NC,\text{eff}} = V_{NC}\bar{\nu}_x\nu_x, \tag{3.4}$$

where V_{NC} is independent of the neutrino flavor ν_x. For anti-neutrinos, the signs of the effective potentials change.

From the above it follows that, in the quantum mechanical description of neutrino oscillations, the effective Hamiltonian H' in matter is given by

$$H' = H'_{\text{kin}} + H_{CC,\text{eff}} + H_{NC,\text{eff}}, \tag{3.5}$$

where $H'_{\rm kin}$ is defined by its representation in the mass basis which is given by H_m of Eq. (2.19),

$$H_{CC,{\rm eff},f} = \begin{pmatrix} V_{CC} & 0 & \dots \\ 0 & 0 & \dots \\ \vdots & \vdots & \ddots \end{pmatrix}, \tag{3.6}$$

and $H_{NC,{\rm eff},f} = V_{NC}\mathbf{1}$, where $\mathbf{1}$ is the identity matrix. As in the case of vacuum oscillations, any part of the Hamiltonian which is proportional to the identity operator only contributes with an overall phase factor which does not affect the oscillation probabilities and may be dropped. We therefore define a new Hamiltonian H by subtracting $(p + \frac{m_1^2}{2p} + V_{NC})\mathbf{1}$ from H' and the result is

$$H = H_{\rm kin} + H_{CC,{\rm eff}}, \tag{3.7}$$

where $H_{\rm kin}$ is expressed as

$$H_{{\rm kin},m} = \frac{1}{2p}\begin{pmatrix} 0 & 0 & 0 & \dots \\ 0 & \Delta m^2_{21} & 0 & \dots \\ 0 & 0 & \Delta m^2_{31} & \dots \\ \vdots & \vdots & \vdots & \ddots \end{pmatrix} \tag{3.8}$$

in the mass basis, and $H_{CC,{\rm eff}}$ is given by Eq. (3.6). In the flavor and mass bases, H is given by $H_f = UH_{{\rm kin},m}U^\dagger + H_{CC,{\rm eff},f}$ and $H_m = H_{{\rm kin},m} + U^\dagger H_{CC,{\rm eff},f}U$, respectively.

For a non-zero V_{CC}, the eigenstates of the Hamiltonian H are not the same as the mass eigenstates. For matter effects, it is useful to define the matter eigenstate basis $M = \{|\nu_{M,i}\rangle\}$, where $H|\nu_{M,i}\rangle = E_i|\nu_{M,i}\rangle$. Just as in the case of vacuum neutrino oscillations, we can relate the basis M to the flavor basis by a unitary transformation $\hat{U}$, the matter mixing matrix, such that

$$|\nu\rangle_f = \hat{U}|\nu\rangle_M . \tag{3.9}$$

For vacuum oscillations, the basis M coincides with the mass eigenstate basis, and thus, we have $\hat{U} = U$.

3.2 Majorana neutrinos in matter

As we noticed in Sec. 2.6, it is impossible to distinguish between Majorana and Dirac neutrinos through neutrino oscillations in vacuum. This clearly raises the

question whether the distinction can be made in the case of matter effects or not. The Hamiltonian is expressed in flavor basis as

$$H_f = U H_{\text{kin},m} U^\dagger + H_{CC,\text{eff},f} = U^{\text{D}} D H_{\text{kin},m} D^\dagger U^{\text{D}\dagger} + H_{CC,\text{eff},f}, \tag{3.10}$$

where we have adopted the notation of Sec. 2.6. Since both $H_{\text{kin},m}$ and D are diagonal matrices, they commute, and thus, we have

$$H_f = U^{\text{D}} H_{\text{kin},m} U^{\text{D}\dagger} + H_{CC,\text{eff},f}, \tag{3.11}$$

which is the same Hamiltonian as in the case of Dirac neutrinos. It follows that, as in the case of vacuum oscillations, Majorana and Dirac neutrinos are indistinguishable through neutrino oscillations in matter.

3.3 Matter effects in two flavor neutrino oscillations

In the case of two flavor neutrino oscillations in matter, the Hamiltonian is given by

$$H_f = \begin{pmatrix} V_{CC} + \frac{\Delta m^2}{2E} s^2 & \frac{\Delta m^2}{2E} sc \\ \frac{\Delta m^2}{2E} sc & \frac{\Delta m^2}{2E} c^2 \end{pmatrix} \text{ or } H_m = \begin{pmatrix} V_{CC} c^2 & V_{CC} sc \\ V_{CC} sc & V_{CC} s^2 + \frac{\Delta m^2}{2E} \end{pmatrix}, \tag{3.12}$$

where we use the standard parameterization and notation of Eq. (2.23). It is useful to subtract $\frac{\Delta m^2}{2p}\mathbf{1}$ from this Hamiltonian, since this, as we have noted before, does not change the oscillation probabilities. The Hamiltonian expressed in flavor basis is then given by

$$H_f = \begin{pmatrix} -\frac{\Delta m^2}{4E}\cos(2\theta) + V_{CC} & \frac{\Delta m^2}{4E}\sin(2\theta) \\ \frac{\Delta m^2}{4E}\sin(2\theta) & \frac{\Delta m^2}{4E}\cos(2\theta) \end{pmatrix}. \tag{3.13}$$

The matter mixing matrix $\hat{U}$ that diagonalizes H_f can be parameterized in the same way as U, the parameter angle is denoted by $\hat{\theta}$ and known as the "mixing angle in matter".

3.3.1 Constant density

Let us first consider the rather simple case of neutrino oscillations in matter with constant density, or rather, constant electron number density N_e. In this case,

also the effective CC potential V_{CC} is constant in time and by performing the diagonalization of H_f, we obtain

$$\tan(2\hat{\theta}) = \frac{\frac{\Delta m^2}{2E}\sin(2\theta)}{\frac{\Delta m^2}{2E}\cos(2\theta) - V_{CC}}, \tag{3.14}$$

where we can clearly observe that $\hat{\theta} = \theta$ for $V_{CC} = 0$, i.e., for vacuum oscillations. Basically, we have the same calculations as in the case of vacuum oscillation with the substitution of $\theta \to \hat{\theta}$ and the resulting oscillation probability is given by

$$P_{ex}(L) = \sin^2(2\hat{\theta})\sin^2\left(\frac{\Delta E}{2}L\right) = \sin^2(2\hat{\theta})\sin^2\left(\frac{\pi L}{L_{\mathrm{osc},M}}\right), \tag{3.15}$$

where ΔE is the difference in energy of the two eigenstates of the Hamiltonian and $L_{\mathrm{osc},M} = \frac{2\pi}{\Delta E}$ is the oscillation length in matter. Solving the second order eigenvalue equation for the Hamiltonian, we find the energy difference as

$$\Delta E = \sqrt{\left(\frac{\Delta m^2}{2E}\cos(2\theta) - V_{CC}\right)^2 + \left(\frac{\Delta m^2}{2E}\right)^2 \sin^2(2\theta)}. \tag{3.16}$$

Using the trigonometric identity $\sin^2\beta = \frac{\tan^2\beta}{1+\tan^2\beta}$, we obtain

$$\sin^2(2\hat{\theta}) = \frac{\left(\frac{\Delta m^2}{2E}\right)^2 \sin^2(2\theta)}{\left(\frac{\Delta m^2}{2E}\cos(2\theta) - V_{CC}\right)^2 + \left(\frac{\Delta m^2}{2E}\right)^2 \sin^2(2\theta)} \tag{3.17}$$

for the oscillation amplitude $\sin^2(2\hat{\theta})$. Note that when

$$V_{CC} = \frac{\Delta m^2}{2E}\cos(2\theta), \tag{3.18}$$

then $\sin^2(2\hat{\theta}) = 1$ and the oscillation probability varies from zero to one. The condition in Eq. (3.18) is the so-called Mikheyev-Smirnov-Wolfenstein (MSW) resonance condition and when it is fulfilled, the mixing angle in matter becomes maximal ($\hat{\theta} = 45°$).

For neutrinos, the left-hand side of Eq. (3.18) is positive, and thus, the right-hand side must be positive if there is to be a resonance. Usually, one uses the convention $\cos(2\theta) > 0$, which is always possible by reordering the mass eigenstates. Thus, there is no resonance for neutrino oscillations if not $\Delta m^2 > 0$. For anti-neutrinos, the argument is reversed, since the effective potential V_{CC} changes sign, and if the resonance condition is to be fulfilled for anti-neutrinos, then we need $\Delta m^2 < 0$.

3.3.2 Varying density

In the case of constant electron number density, we could perform our calculations in the same manner as in the case of vacuum oscillations, using the matter eigenstates in place of the mass eigenstates. However, when the electron number density is not constant, the matter eigenstates will not be constant in time and we cannot use the same formalism as in the vacuum case. The change of the matter eigenstates with time will lead to transitions from $|\nu_{1,M}\rangle$ to $|\nu_{2,M}\rangle$ and vice versa. The Schrödinger equation in the matter eigenstate basis, which changes in time, can be deduced as

$$\mathrm{i}\frac{\mathrm{d}\,|\nu\rangle_M}{\mathrm{d}t} = \mathrm{i}\frac{\mathrm{d}(\hat{U}^\dagger\,|\nu\rangle_f)}{\mathrm{d}t} = \mathrm{i}\hat{U}^\dagger\frac{\mathrm{d}\,|\nu\rangle_f}{\mathrm{d}t} + \mathrm{i}\frac{\mathrm{d}\hat{U}^\dagger}{\mathrm{d}t}\,|\nu\rangle_f = (H_M - \mathrm{i}\hat{U}^\dagger\frac{\mathrm{d}\hat{U}}{\mathrm{d}t})\,|\nu\rangle_M\,, \quad (3.19)$$

where we have used the Schrödinger equation in flavor basis and $H_M = \hat{U}^\dagger H_f \hat{U}$. Note that Eq. (3.19) holds in the general case with n neutrino flavors and that $\hat{U}^\dagger\frac{\mathrm{d}\hat{U}}{\mathrm{d}t}$ is always traceless.

For the case of two neutrino flavors, Eq. (3.19) reads

$$\mathrm{i}\frac{\mathrm{d}\,|\nu\rangle_M}{\mathrm{d}t} = \begin{pmatrix} E_1 & -\mathrm{i}\dot{\hat{\theta}} \\ \mathrm{i}\dot{\hat{\theta}} & E_2 \end{pmatrix}|\nu\rangle_M\,, \quad (3.20)$$

where E_1 and E_2 are the energies of the matter eigenstates. From this equation, it is clear that transitions between the matter eigenstates are induced by the change of the mixing angle in matter, $\hat{\theta}$. When the electron number density changes slowly, $\dot{\hat{\theta}}$ will be small and the transitions between different matter eigenstates will be suppressed. The so-called "adiabatic" approximation makes this assumption, and in this approximation, the matter eigenstates evolve separately. The condition that must be fulfilled for the adiabatic approximation to be a good approximation is that the adiabaticity parameter

$$\gamma = \frac{|\Delta E|}{2\dot{\hat{\theta}}} \quad (3.21)$$

fulfills the condition $\gamma \gg 1$.

In the adiabatic approximation, we neglect the off-diagonal elements in Eq. (3.20) and the time evolution is such that the matter eigenstates just receive phase factors, namely

$$\phi_i^M(t) = \exp\left(-\mathrm{i}\int_0^t E_i(\tau)\mathrm{d}\tau\right)\phi_i^M(0). \quad (3.22)$$

Thus, if the adiabaticity condition holds, then the oscillation probability $P_{ex}(t)$ is given by

$$\begin{aligned} P_{ex}(t) &= \left| \begin{pmatrix} -\sin\hat{\theta}(t) & \cos\hat{\theta}(t) \end{pmatrix} \begin{pmatrix} \phi_1^M(t) \\ \phi_2^M(t) \end{pmatrix} \right|^2 \\ &= \frac{1}{2} - \frac{1}{2}\cos(2\hat{\theta}(t))\cos(2\hat{\theta}(0)) \\ &\quad -\frac{1}{2}\sin(2\hat{\theta}(t))\sin(2\hat{\theta}(0))\cos(\varphi_1 - \varphi_2), \end{aligned} \tag{3.23}$$

where

$$\varphi_i = \int_0^t E_i(\tau)\mathrm{d}\tau. \tag{3.24}$$

If the production or detection regions are large compared to the corresponding oscillation lengths, then the $\cos(\varphi_1 - \varphi_2)$ term will effectively be averaged out, and the oscillation probability is then given by

$$P_{ex}(t) = \frac{1}{2} - \frac{1}{2}\cos(2\hat{\theta}(0))\cos(2\hat{\theta}(t)). \tag{3.25}$$

We should note that if we produce electron neutrinos at a point with an electron number density far above the MSW resonance (so that $\cos(2\hat{\theta}(0)) \simeq -1$), which propagates adiabatically to vacuum, then the oscillation probability is given by

$$P_{ex} = \frac{1}{2} + \frac{1}{2}\cos(2\theta). \tag{3.26}$$

This is quite remarkable, since we can obtain a large conversion of electron neutrinos even for small mixing angles. This effect is known as the MSW effect. However, for small enough values of θ the adiabaticity condition will always be violated.

The energy gap ΔE obtains its smallest value at the resonance and by differentiating Eq. (3.17), we obtain

$$\dot{\hat{\theta}} = \frac{\frac{\Delta m^2}{2E}\sin(2\theta)\dot{V}_{CC}}{\left(\frac{\Delta m^2}{2E}\cos(2\theta) - V_{CC}\right)^2 + \left(\frac{\Delta m^2}{2E}\right)^2 \sin^2(2\theta)}, \tag{3.27}$$

which shows that if $\dot{V}_{CC}$ is fairly constant in the region around the resonance, then $|\dot{\hat{\theta}}|$ obtains its maximal value at the resonance. It follows that the adiabaticity condition $\gamma \gg 1$ is violated at the resonance if it is violated at any other point. The adiabaticity parameter at the resonance is given by

$$\gamma_{\mathrm{res}} = \frac{\left(\frac{\Delta m^2}{2E}\right)^2 \sin^2(2\theta)}{|\dot{V}_{CC}|_{\mathrm{res}}} = \frac{\frac{\Delta m^2}{2E}\sin^2(2\theta)}{\cos(2\theta)} \left|\frac{V_{CC}}{\dot{V}_{CC}}\right|_{\mathrm{res}}, \tag{3.28}$$

where we have used that $V_{CC} = \frac{\Delta m^2}{2E}\cos(2\theta)$ at the resonance.

Let us suppose that the adiabaticity condition is violated in a region near the resonance and that there is some probability $P_{\rm jump}$ of transition between the matter eigenstates. The averaged flavor transition probability is then given by

$$P_{ex}(t) = \frac{1}{2} - \frac{1}{2}\cos(2\hat{\theta}(0))\cos(2\hat{\theta}(t))(1 - 2P_{\rm jump}). \tag{3.29}$$

If we use a linear approximation of the effective potential V_{CC} near the resonance, then $P_{\rm jump}$ is given by [43]

$$P_{\rm jump} = e^{-\frac{\pi}{2}\gamma_{\rm res}}. \tag{3.30}$$

Observe that $P_{\rm jump} \to 0$ as $\gamma_{\rm res} \to \infty$, i.e., $P_{\rm jump} = 0$ in the adiabatic limit just as should be expected.

3.4 Matter effects in three flavor neutrino oscillations

As in the case of three flavor neutrino oscillations in vacuum, there is no simple analytical expression for the oscillation probabilities for three flavor neutrino oscillations in matter. As in the case of two flavor neutrino oscillations, we use the same parameterization of the leptonic mixing matrix in matter as for the leptonic mixing matrix in vacuum and we denote the matter mixing parameters by $\hat{a}$, where a is the corresponding vacuum parameter. The 3×3 Hamiltonian in matter is most easily expressed in the mass eigenstate basis in which it is given by

$$\begin{aligned} H_m &= \begin{pmatrix} V_{CC}|U_{e1}|^2 & V_{CC}U^*_{e1}U_{e2} & V_{CC}U^*_{e1}U_{e3} \\ V_{CC}U^*_{e2}U_{e1} & V_{CC}|U_{e2}|^2 + \frac{\Delta m^2_{21}}{2E} & V_{CC}U^*_{e2}U_{e3} \\ V_{CC}U^*_{e3}U_{e1} & V_{CC}U^*_{e3}U_{e2} & V_{CC}|U_{e3}|^2 + \frac{\Delta m^2_{31}}{2E} \end{pmatrix} \\ &= \begin{pmatrix} 0 & 0 & 0 \\ 0 & K_1 & 0 \\ 0 & 0 & K_2 \end{pmatrix} + \\ &\quad V_{CC} \begin{pmatrix} c^2_{13}c^2_{12} & c^2_{13}s_{12}c_{12} & c_{13}s_{13}c_{12}e^{\mathrm{i}\delta} \\ c^2_{13}s_{12}c_{12} & c^2_{13}s^2_{12} & c_{13}s_{13}s_{12}e^{\mathrm{i}\delta} \\ c_{13}s_{13}c_{12}e^{-\mathrm{i}\delta} & c_{13}s_{13}s_{12}e^{-\mathrm{i}\delta} & s^2_{13} \end{pmatrix}, \end{aligned} \tag{3.31}$$

where $K_1 = \frac{\Delta m^2_{21}}{2E}$ and $K_2 = \frac{\Delta m^2_{31}}{2E}$. This Hamiltonian is independent of the mixing angle θ_{23}, which means that the propagation of the mass eigenstates will not depend on θ_{23}.

There are a few things which differ significantly from the two flavor oscillations in matter to the three flavor oscillations in matter. First of all, there are now three different energy eigenstates $|\nu_{i,M}\rangle$ of the Hamiltonian at any given point. In general, according to what we have learned from the two flavor oscillations, one would think that this allows for three different resonances, where the energy

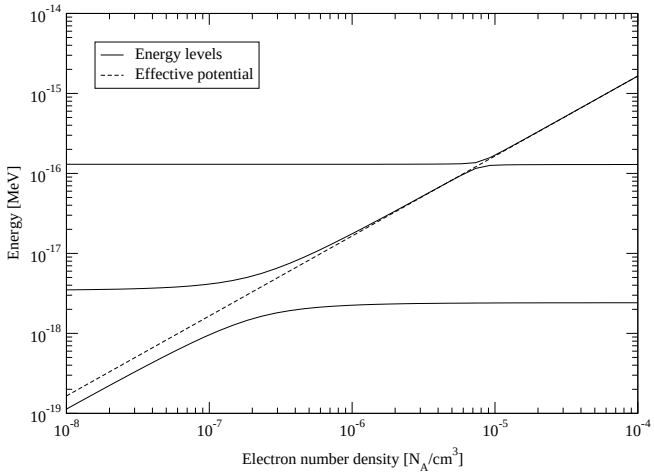

Figure 3.2. Neutrino energy levels as a function of the matter density at neutrino momentum $p = 10$ MeV. The best-fit values of Table 3.2 has been used for the oscillation parameters.

gap between different energy eigenstates is minimal, we will have three different energy gaps $\Delta E_{ij} = E_i - E_j$ and three adiabaticity parameters $\gamma_{ij} = \frac{|(\dot{H}_M)_{ij}|}{\Delta E_{ij}}$ to consider. However, since the middle energy level is always inbetween the lowest and the highest energy levels, we will have $\Delta E_{31} \geq \frac{\Delta m^2_{32}}{2E}$. To leading order Feynman diagrams, the NC interactions are independent of the charged fermion masses and two asymptotes of the energy levels will be parallel, which means that we will have two resonances only, see Fig. 3.2. However, in higher order Feynman diagrams, the NC interactions are not the same for different neutrino flavors. In this case, there is an additional resonance between the middle energy level and the highest energy level. If the two previous resonances occur for neutrinos, this additional resonance occurs for anti-neutrinos and vice-versa. Also, the matter densities involved in this resonance are much higher than those involved for the two other resonances, for details see Ref. [44].

In what follows, we will assume the mass squared difference hierarchy given in Eq. (2.30). This hierarchy can be constructed in two different ways, either we have a "normal" mass hierarchy such that $m_1 \lesssim m_2 \ll m_3$ or an "inverted" mass hierarchy such that $m_3 \ll m_1 \lesssim m_2$. Experiments have determined that $m_1 < m_2$, which means that Δm^2_{21} is positive. However, the sign of the mass squared difference Δm^2_{31} is still to be determined. If Δm^2_{31} is negative, then the resonance due to this mass squared difference will occur for anti-neutrinos and not neutrinos. From

the two flavor case, we expect the resonances of the three flavor case to occur for an effective potential of $V_{CC} \sim \frac{\Delta m^2_{21}}{2E}$ and $V_{CC} \sim \frac{\Delta m^2_{31}}{2E}$, respectively. We start by examining the case of $V_{CC} \sim \frac{\Delta m^2_{21}}{2E} \ll \frac{\Delta m^2_{31}}{2E}$. In this case, the third element of the third row in the Hamiltonian of Eq. (3.31) will be much larger than any other element of the Hamiltonian and the matter eigenstate $|\nu_{3,M}\rangle$ is then approximately equal to the mass eigenstate $|\nu_3\rangle$. Making the approximation that $|\nu_3\rangle$ evolves as in vacuum yields for the remaining mass eigenstate components

$$\mathrm{i}\frac{\mathrm{d}}{\mathrm{d}t}\begin{pmatrix}\phi_1\\ \phi_2\end{pmatrix} = \left[c^2_{13}V_{CC}\begin{pmatrix} c^2_{12} & s_{12}c_{12}\\ s_{12}c_{12} & s^2_{12}\end{pmatrix} + \begin{pmatrix}0 & 0\\ 0 & K_1\end{pmatrix}\right]\begin{pmatrix}\phi_1\\ \phi_2\end{pmatrix}. \tag{3.32}$$

Comparing this equation with Eq. (3.12), we note that this exactly corresponds to the evolution in the case of two neutrino flavors with $\theta = \theta_{12}$ and using $c^2_{13}V_{CC}$ for the effective potential. Observe that this holds for the mass eigenstates and not necessarily for the flavor eigenstates, since these are linear combinations of mass eigenstates and $|\nu_3\rangle$ is, in general, not a flavor eigenstate. Following the calculations of the two flavor case, we obtain the resonance condition

$$c^2_{13}V_{CC} = \frac{\Delta m^2_{21}}{2E}\cos(2\theta_{12}), \tag{3.33}$$

and the probability

$$P_{\mathrm{jump},12} = e^{-\frac{\pi}{2}\gamma_{\mathrm{res},12}} = \exp\left(-\frac{\pi\Delta m^2_{21}\sin^2(2\theta_{12})}{4E\cos(2\theta_{12})}\left|\frac{V_{CC}}{\dot{V}_{CC}}\right|_{\mathrm{res}}\right) \tag{3.34}$$

of a transition from the matter eigenstate $|\nu_{1,M}\rangle$ to the matter eigenstate $|\nu_{2,M}\rangle$ or vice versa. We also obtain that $P_{\mathrm{jump},12}$ is independent of θ_{13}, since the effective potential enters only in $\left|\frac{V_{CC}}{\dot{V}_{CC}}\right|$.

Next we examine the case when $V_{CC} \sim \frac{\Delta m^2_{31}}{2E} \gg \frac{\Delta m^2_{21}}{2E}$. In this case, $K_1 = \frac{\Delta m^2_{21}}{2E}$ may be neglected in a first approximation. We introduce a new basis $B = \{|\nu_{i,B}\rangle\}$ by relating this new basis to the mass eigenstates by the unitary transformation $|\nu\rangle_B = V\,|\nu\rangle_m$, where

$$V = \begin{pmatrix} c_{12} & s_{12} & 0\\ -s_{12} & c_{12} & 0\\ 0 & 0 & e^{\mathrm{i}\delta}\end{pmatrix}, \tag{3.35}$$

the Hamiltonian is then given by

$$H_B = \begin{pmatrix} V_{CC}c^2_{13} & 0 & V_{CC}s_{13}c_{13}\\ 0 & 0 & 0\\ V_{CC}s_{13}c_{13} & 0 & V_{CC}s^2_{13} + K_2\end{pmatrix}. \tag{3.36}$$

The state $|\nu_{B,2}\rangle$ is clearly an eigenstate of this Hamiltonian (it corresponds to the matter eigenstate $|\nu_{1,M}\rangle$) and this state evolves independently of the two others.

The calculations that follow for the second and third matter eigenstates are the same as for the two flavor oscillations in matter with $\theta = \theta_{13}$. The resonance condition is

$$V_{CC} = \frac{\Delta m^2_{31}}{2E}\cos(2\theta_{13}), \tag{3.37}$$

and the probability of a transition between the second and third matter eigenstates is given by

$$P_{\text{jump},23} = e^{-\frac{\pi}{2}\gamma_{\text{res},23}} = \exp\left(-\frac{\pi\Delta m^2_{31}\sin^2(2\theta_{13})}{4E\cos(2\theta_{13})}\left|\frac{V_{CC}}{\dot{V}_{CC}}\right|_{\text{res}}\right). \tag{3.38}$$

Now, suppose that we produce electron neutrinos and that the effective potential of the matter density at the point of production is $V_{\text{prod}} = \sqrt{2}G_F N_{e,\text{prod}}$. We then let the neutrinos propagate adiabatically between the resonances, have a probability $P_{\text{jump},ij}$ of jumping from $|\nu_{i,M}\rangle$ to $|\nu_{j,M}\rangle$ at the resonance involving the ith and the jth matter eigenstate, and end up in vacuum. If we denote the averaged probability of finding the neutrinos in the mass eigenstate $|\nu_i\rangle$ after the propagation described above by P_{ei}, then

$$P_{ei} = \sum_{j=1}^{3}|U_{ej}|^2 P_{ji}, \tag{3.39}$$

where P_{ji} is the averaged probability of a neutrino of the matter eigenstate $|\nu_{j,M}\rangle$ to evolve into the mass eigenstate $|\nu_i\rangle$. If we suppose that $V_{\text{prod}} > \frac{\Delta m^2_{31}}{2E}\cos(2\theta_{13})$, then the neutrinos pass both resonances and the P_{ji}'s are well approximated by

$$\begin{aligned} P_{11} &= 1 - P_{\text{jump},12}, \\ P_{23} &= P_{\text{jump},23}, \\ P_{31} &= P_{\text{jump},12}P_{\text{jump},23}, \\ P_{33} &= 1 - P_{\text{jump},23}, \end{aligned} \tag{3.40}$$

and

$$\sum_{i=1}^{3} P_{ji} = 1, \quad \sum_{j=1}^{3} P_{ji} = 1. \tag{3.41}$$

If neutrinos are produced at a point such that the inequalities $\frac{\Delta m^2_{21}}{c^2_{13}2E}\cos(2\theta_{12}) < V_{\text{prod}} < \frac{\Delta m^2_{31}}{2E}\cos(2\theta_{13})$ hold, then the neutrinos only pass the lower resonance and the P_{ij}'s are given by

$$\begin{aligned} P_{3i} &= \delta_{3i}, \\ P_{j3} &= \delta_{j3}, \\ P_{12} &= P_{\text{jump},12}, \end{aligned} \tag{3.42}$$

and Eq. (3.41). If the neutrino production occur in a region such that $V_{\text{prod}} < \frac{\Delta m^2_{21}}{c^2_{13}2E}\cos(2\theta_{12})$, then the entire evolution is adiabatic and we obtain $P_{ij} = \delta_{ij}$. If Δm^2_{31} is negative, then neutrinos can pass at most one resonance.

Name	Reaction
pp	$p + p \rightarrow d + e^+ + \nu_e$
pep	$p + p + e^- \rightarrow d + \nu_e$
hep	$^3\mathrm{He} + p \rightarrow {}^4\mathrm{He} + e^+ + \nu_e$
^{7}Be	$^7\mathrm{Be} + e^- \rightarrow {}^7\mathrm{Li} + \nu_e$
^{8}B	$^8\mathrm{B} \rightarrow {}^8\mathrm{Be}^* + e^+ + \nu_e$

Table 3.1. The reactions which produce the main part of the solar neutrinos.

3.5 The solar neutrino problem

3.5.1 The standard solar model

The standard solar model (SSM) [24] is a model describing the Sun. According to the SSM, electron neutrinos are produced in the Sun mainly through the reactions in Table 3.1. In Fig. 3.3, the SSM prediction of the electron neutrino flux is shown as a function of the neutrino energy E_ν, the figure also includes the energy thresholds for which different experiments measure neutrinos. In addition, the SSM predicts the electron number density of the Sun as well as the spatial distribution of the neutrino production for each separate reaction, the spatial production distribution of ^{8}B neutrinos is shown in Fig. 3.4. Supposing that electron neutrinos originating from thermonuclear reactions in the Sun reach the Earth as electron neutrinos, the SSM can predict the detection rates at different experimental facilities. Data on the SSM can be retrieved from Ref. [45]. As a final note, we should remark that the SSM is not the only solar model available, see for example Ref. [46].

3.5.2 The solar neutrino experiments

A number of experiments have been performed to measure the flux of solar electron neutrinos. The first of these was the Homestake experiment [47] in which neutrinos are detected by the reaction

$$\nu_e + {}^{37}\mathrm{Cl} \rightarrow {}^{37}\mathrm{Ar} + e^-. \tag{3.43}$$

The argon atoms produced through this reaction are radioactive and can be extracted through chemical methods and then counted in proportional counters. As can be seen in Fig. 3.3, the Homestake experiment, which is a "chlorine" experiment, could not observe the neutrinos produced in the pp-reaction. However, the pp-neutrinos can be detected in experiments similar to the Homestake experiment. The SAGE [48] and Gallex [49] experiments also uses radiochemical methods to measure the flux of the solar electron neutrinos, but instead of the reaction given in Eq. (3.43), the reaction

$$\nu_e + {}^{71}\mathrm{Ga} \rightarrow {}^{71}\mathrm{Ge} + e^- \tag{3.44}$$

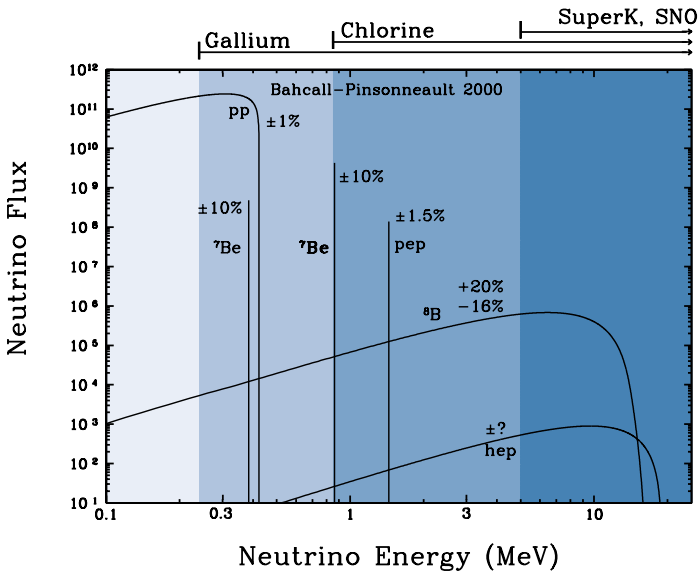

Figure 3.3. The contributions to the solar neutrino flux according to the SSM. The figure is retrieved from Ref. [45].

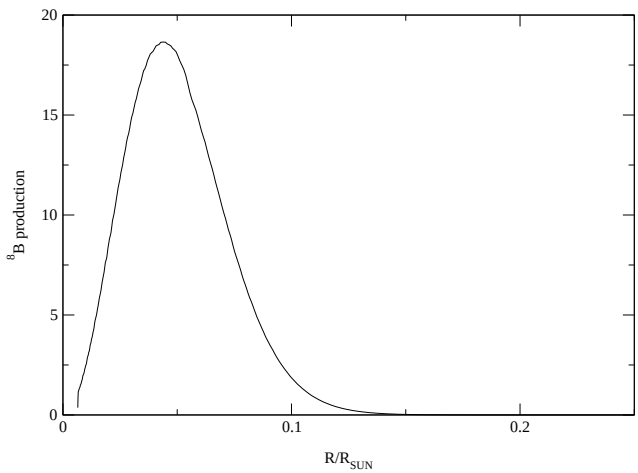

Figure 3.4. The production distribution of ^{8}B neutrinos in the Sun according to the SSM. The data are retrieved from Ref. [45]

is used. This reaction has a threshold energy of 0.234 MeV, and thus, a large part of the neutrinos produced in the pp-reaction can be detected in these experiments.

None of the above experiments can detect the specific energy of the solar neutrinos, nor detect the solar neutrinos in real-time, since the radiochemical detection of the produced radioactive nuclei is not immediate. Both of these features are implemented in the water-Cherenkov detectors of Super-Kamiokande (SK) and the Sudbury Neutrino Observatory (SNO). Both SK and SNO use the elastic scattering reaction

$$\nu_e + e^- \rightarrow \nu_e + e^- \tag{3.45}$$

to detect neutrinos, the Cherenkov light produced by and, indirectly, the energy of the scattered electron is measured by photo multipliers. This gives real-time detection of neutrino events as well as some information about the neutrino energy and direction. However, to avoid background events, the threshold energy is set to 5 MeV, and thus, the main part of the neutrinos detected are produced in the ^{8}B reaction. At SK, the water used in the detector is ordinary water. However, at SNO, heavy water is used, which also allows for the reactions

$$\nu_e + d \rightarrow p + p + e^-, \tag{3.46}$$

$$\nu_x + d \rightarrow p + n + \nu_x, \tag{3.47}$$

which are known as the charged-current (CC) reaction and the neutral-current (NC) reaction, respectively. The CC reaction is possible only for electron neutrinos, whereas the NC reaction is possible for all types of neutrinos with the same cross-section to leading order in the weak coupling constant. The NC reaction is detected by measuring characteristic photons from neutron capture. In the CC reaction, the main part of the neutrino energy, which is not needed to split the deutron into two protons, is carried away as kinetic energy of the electron.

The results of the measurements of the solar neutrino flux is shown in Fig. 3.5. As can be seen from this figure, there is a discrepancy between the fluxes predicted by the SSM and the fluxes measured in all experiments except for the NC flux at SNO, which is in excellent agreement with the predicted flux [32]. This discrepancy is known as the "solar neutrino problem".

3.5.3 The solution to the solar neutrino problem

Before the measurement of the NC reaction at SNO, a large number of different solutions to the solar neutrino problem were proposed, for example, oscillations into sterile (non-interacting) neutrinos and that the SSM may be incorrect. After the SNO's NC measurement [32], it is quite clear that the discrepancy in the other experiments is due to oscillations of electron neutrinos into other active neutrino flavors. Until recently, there have been four regions of the parameter space θ-Δm^2, which have been presented as possible solutions to the solar neutrino problem (assuming oscillations of electron neutrinos into other neutrino flavors). The first of these regions, known as the vacuum oscillation (VO) solution, involved a small

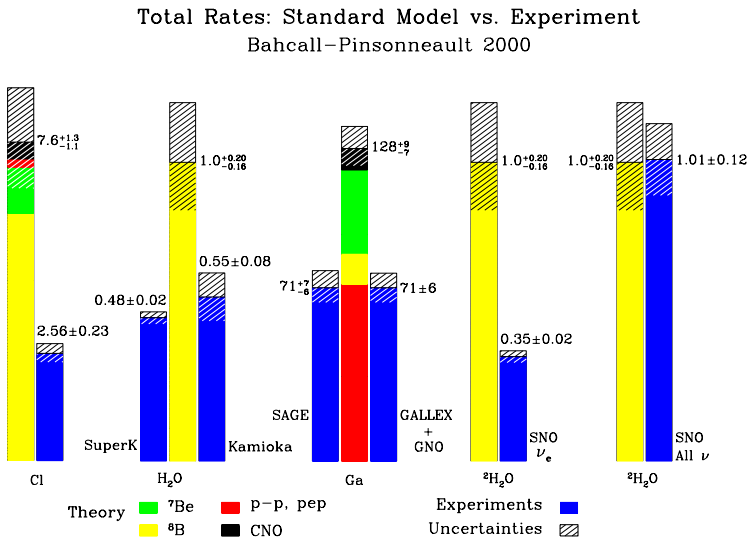

Figure 3.5. The results of the measurements of the solar neutrino flux. The figure is retrieved from Ref. [45].

Parameter	Best-fit	3σ confidence
Δm^2_{21} [10^{-5} eV^2]	6.9	5.4-9.5
$\lvert\Delta m^2_{31}\rvert$ [10^{-3} eV^2]	2.6	1.5-3.7
θ_{12}	33.2°	28.6°-38.6°
θ_{23}	43.9°	$\geq 31.9°$
θ_{13}	4.4°	$\leq 13.4°$

Table 3.2. Best global fits and 3σ confidence intervals of the neutrino parameters according to Ref. [51].

mass squared difference of $\Delta m^2 = \Delta m^2_{21} \sim 10^{-10}$ eV^2 and a mixing angle θ_{12} such that $0.6 \lesssim \sin^2(2\theta_{12}) \lesssim 1$. In this solution, the deficit in the solar electron neutrino flux is due to vacuum oscillations of neutrinos in the region between the Sun and the Earth. This solution is also known as the "just so" solution, since it "just so happens" that the Earth is located at a distance such that most of the electron neutrinos oscillate into other flavors.

The second and third solutions are the small mixing angle (SMA) and large mixing angle (LMA) MSW solutions. These solutions are both based on neutrinos passing a MSW resonance when propagating from the point of production in the Sun to the Earth. The SMA solution involved a small mass squared difference of about $\Delta m^2 \sim 5 \cdot 10^{-6}$ eV^2 and a mixing angle such that $10^{-3} \lesssim \sin^2(2\theta_{12}) \lesssim 10^{-2}$, while the LMA solution involved a small mass squared difference of about $\Delta m^2 \sim 7 \cdot 10^{-5}$ eV^2 and a mixing angle such that $0.65 \lesssim \sin^2(2\theta_{12}) \lesssim 0.97$.

The last solution region is the so-called low mass squared difference (LOW) region, which is also an MSW solution. This solution corresponds to a mass squared difference value of $\Delta m^2 \sim 10^{-7}$ eV^2, which is lower than the value for the other MSW solutions, hence the name. The mixing angle of the LOW solution is near maximal.

Before the SNO experiment, the best-fit was found in the SMA solution region. However, with the inclusion of the SNO results, the best fit was shifted to the LMA region. The results of the KamLAND experiment [50] leave only the LMA solution and global fits performed on newly released data [51] have constrained the size of this region as well as rejected the hypothesis of maximal solar mixing angle ($\theta_{12} = 45°$) at a 5σ confidence level. The best-fits of the fundamental parameters given in Ref. [51] are quoted in Table 3.2.

Chapter 4

The day-night effect

The matter effect on neutrino propagation leads us to the question if the electron neutrino flux from the Sun is changed when passing through the Earth. As will be shown in this chapter, there may well be such an effect leading to a day-night asymmetry in the event rates of solar neutrinos at neutrino detectors. This asymmetry is defined as

$$A_{n-d} = 2\frac{N-D}{N+D}, \tag{4.1}$$

where N and D are the night and day rates, respectively. To observe this asymmetry, real-time detection of neutrino events is needed to determine the zenith angle of the event. As a result, the only current experimental facilities of interest are the Sudbury Neutrino Observatory (SNO) and Super-Kamiokande (SK) experiments. Throughout this chapter, we will assume that the neutrino flux reaching the Earth is incoherent. The motivation for this will be found in Sec. 4.4.

4.1 The day-night asymmetry with n neutrino flavors

Using the assumption of an incoherent neutrino flux, the solar ν_e survival probability is

$$P_S = \sum_{i=1}^{n} k_i |\langle \nu_e | \nu_i \rangle|^2 = \sum_{i=1}^{n} k_i |U_{ei}|^2, \tag{4.2}$$

where n is the number of neutrino flavors and k_i is the fraction of the mass eigenstate $|\nu_i\rangle$ in the flux of solar neutrinos arriving at the Earth. Unitarity implies that

$$\sum_{i=1}^{n} k_i = 1. \tag{4.3}$$

For neutrinos reaching the Earth during daytime (at the detector site), P_S is the ν_e survival probability at the detector. However, during nighttime this survival probability may be altered by the influence of the effective Earth matter potential. Thus, the ν_e survival probability becomes

$$P_{SE} = \sum_{i=1}^{n} k_i |\, \langle \nu_e | \tilde{\nu_i} \rangle \,|^2, \tag{4.4}$$

where $|\tilde{\nu_i}\rangle = |\nu_i(L)\rangle$ (L is the length of the neutrino path through the Earth). Here, the components of $|\nu_i(t)\rangle$ satisfy the differential equation (see Sec. 2.3)

$$\mathrm{i}\frac{\mathrm{d}\,|\nu_i(t)\rangle_m}{\mathrm{d}t} = H_m\,|\nu_i(t)\rangle_m \tag{4.5}$$

with the initial condition $|\nu_i(0)\rangle = |\nu_i\rangle$ and m refers to the components of the mass eigenstate basis. We could, of course, use any basis, but the mass basis seems to yield the easiest calculations.

The Hamiltonian H is given by Eq. (3.7) and the effective Earth matter potential is given by $V_{CC} = \sqrt{2}G_F N_e$, where G_F is the Fermi coupling constant and N_e is the electron number density. The electron number density is a function of t depending on the Earth matter density profile which is given by the Preliminary Reference Earth Model (PREM) [52]. The term $|\, \langle \nu_e | \tilde{\nu_i} \rangle \,|^2$ can be interpreted as the probability of a neutrino reaching the Earth in the mass eigenstate $|\nu_i\rangle$ to be detected as an electron neutrino after traversing the distance L in the Earth. For notational reasons we define

$$P_{ie} = |\, \langle \nu_e | \tilde{\nu_i} \rangle \,|^2. \tag{4.6}$$

Clearly, $P_{ie}(L=0) = |\, \langle \nu_e | \nu_i \rangle \,|^2 = |U_{ei}|^2$. Furthermore, unitarity implies that

$$\sum_{i=1}^{n} P_{ie} = 1. \tag{4.7}$$

The unitarity conditions imply that if all k_i are equal (i.e., $k_i = \frac{1}{n}$), then $P_{SE} = P_S = \frac{1}{n}$.

4.2 The case of two neutrino flavors

The day-night effect in the two flavor framework has been studied for a long [53]. Using the standard parameterization for the leptonic mixing matrix for the case of two neutrino flavors [see Eq. (2.23)], the survival probability P_S becomes

$$P_S = (1-k_2)\cos^2\theta + k_2 \sin^2\theta = \cos^2\theta - k_2\cos(2\theta), \tag{4.8}$$

where we have used the two neutrino version of Eq. (4.3) to eliminate k_1. Similarly, for the survival probability of neutrinos passing through the Earth, we obtain

$$P_{SE} = (1-k_2)(1-P_{2e}) + k_2 P_{2e} = \frac{1}{2} + 2\left(k_2 - \frac{1}{2}\right)\left(P_{2e} - \frac{1}{2}\right), \tag{4.9}$$

where, in addition to eliminating k_1, we have eliminated P_{1e} by using the unitarity condition given in Eq. (4.7).

Now we use Eq. (4.8) to express k_2 in terms of P_S and θ. Inserting this equation into the expression for P_{SE}, we obtain the well-known expression for the two flavor ν_e survival probability of neutrinos passing through the Earth

$$P_{SE} = P_S + \frac{1 - 2P_S}{\cos(2\theta)}(P_{2e} - \sin^2\theta). \tag{4.10}$$

The difference between P_{SE} and P_S is known as the "regenerative term" and is given by

$$P_{n-d} = P_{SE} - P_S = \frac{1 - 2P_S}{\cos(2\theta)}(P_{2e} - \sin^2\theta). \tag{4.11}$$

Initially, it was argued that there would be no day-night effect for a maximal mixing angle ($\theta = \frac{\pi}{4}$), since this implies that $P_S = \frac{1}{2}$. However, as was shown in Ref. [53], the correct expression to be used in this case is Eq. (4.9), since $\cos(2\theta) = 0$ at maximal mixing. Thus, using the correct expression, there is no reason to expect $P_{n-d} = 0$.

To examine the day-night effect more closely, it is apparent that we need expressions for P_S and P_{2e}. The former is only dependent on the production and propagation of neutrinos within the Sun, while the latter is only dependent on the propagation of neutrinos within the Earth. We start by studying the production and propagation in the Sun and then turn to the Earth effects.

4.2.1 Production and propagation in the Sun

When electron neutrinos are produced in the Sun, they are produced as a linear combination of matter eigenstates given by

$$|\nu_e\rangle = \cos\hat{\theta}\,|\nu_{M,1}\rangle + \sin\hat{\theta}\,|\nu_{M,2}\rangle\,, \tag{4.12}$$

where $\hat{\theta}$ is the mixing angle in matter at the point of production and is a function of the electron number density at that point. Furthermore, the fraction of solar neutrinos arriving at the Earth in the mass eigenstate $|\nu_i\rangle$ is given by

$$k_i = \int_0^{R_\odot} \mathrm{d}r f(r)(\cos^2\hat{\theta}(r)P^s_{1i} + \sin^2\hat{\theta}(r)P^s_{2i}), \tag{4.13}$$

where P^s_{ki} is the probability of a neutrino mass eigenstate $|\nu_{M,k}\rangle$ at position r to exit the Sun in the state $|\nu_i\rangle$. Here, the function f is the normalized distribution function of the production of the neutrinos and we have assumed incoherent transitions.

Using unitarity conditions, we find $P^s_{12} = P^s_{21} = P_{\text{jump}}$ and obtain

$$k_1 = \frac{1 + D_{2\nu}}{2} \ , \quad k_2 = \frac{1 - D_{2\nu}}{2}, \tag{4.14}$$

where

$$D_{2\nu} = \int_0^{R_\odot} \mathrm{d}r f(r) \cos(2\hat{\theta}(r))(1 - 2P_{\text{jump}}). \tag{4.15}$$

In the adiabatic approximation, $P_{\text{jump}} = 0$ and the neutrinos created in the matter eigenstate $|\nu_{M,i}\rangle$ exit the Sun in the mass eigenstate $|\nu_i\rangle$. For the MSW solutions to the solar neutrino problem, an approximate expression for P_{jump} is given by Eq. (3.30) Using the best-fit values of Ref. [51] for the oscillation parameters and that the solar electron number density according to the SSM [45] is approximately given by $N_e(r) \simeq N_e(0)e^{-\frac{r}{r_0}}$, where $r_0 \simeq 0.1R_\odot$, we obtain for a neutrino momentum of 10 MeV

$$\gamma_{\text{res}} \simeq 2.6 \cdot 10^3, \tag{4.16}$$

and thus, $P_{\text{jump}} \sim 10^{-1700}$, which is obviously negligible.

Now, in order to find the survival probability P_S, we insert Eq. (4.14) into Eq. (4.8), which yields

$$P_S = \frac{1}{2}[(1 + D_{2\nu}) \cos^2\theta + (1 - D_{2\nu}) \sin^2\theta] = \frac{1 + D_{2\nu}\cos(2\theta)}{2}. \tag{4.17}$$

4.2.2 Propagation in the Earth

Next, we wish to compute the probability P_{2e} of a neutrino arriving at the Earth in the state $|\nu_i\rangle$ to be in the state $|\nu_e\rangle$ after propagating through the Earth. This depends on the matter density profile of the Earth and Fig. 4.1 shows the so-called Preliminary Reference Earth Model (PREM) profile [52].

We approximate the Earth electron number density profile with a constant density profile [54] with about the average electron density of the Earth crust. This is motivated by the following observations:

- The detectors of interest (SK and SNO) are placed at latitudes such that neutrinos from the Sun rarely pass through the core of the Earth.
- We want to obtain a qualitative understanding of the day-night effect and need the approximation to have a fairly simple analytic behavior.
- The main non-adiabatic process of the neutrino evolution is the neutrino entry into the Earth. The propagation in the Earth will be fairly adiabatic. As we will show, the oscillatory behavior of the regenerative term is averaged out. Thus, the exact nature of the adiabatic propagation is irrelevant as long as the matter potential at the entry into the Earth and at detection are the same and we may just as well use a constant matter potential.

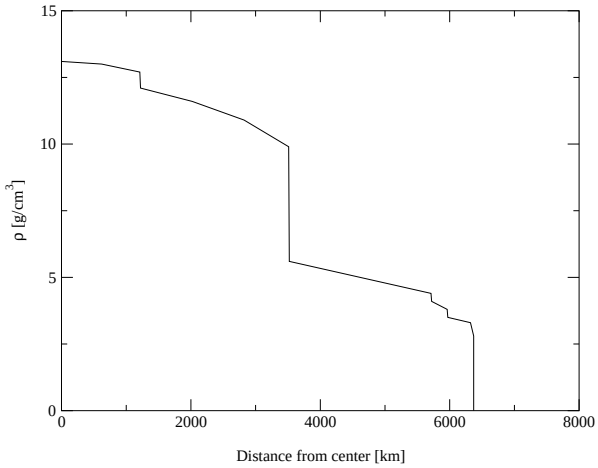

Figure 4.1. The Earth matter density profile as a function of the distance from the center of the Earth according to the PREM [52].

Now the problem of finding P_{2e} reduces to the problem of finding the solution to the differential equation (4.5) with $V_{CC} = V_E = \text{const}$. The Hamiltonian in the mass eigenstate basis becomes

$$H_m = \begin{pmatrix} p + \frac{m_1^2}{2p} & 0 \\ 0 & p + \frac{m_2^2}{2p} \end{pmatrix} + V_E \begin{pmatrix} c^2 & sc \\ sc & s^2 \end{pmatrix}, \tag{4.18}$$

where $s = \sin\theta$ and $c = \cos\theta$. Since the part of the Hamiltonian which is proportional to unity only amounts to multiplying the solution with a phase factor $\exp(i\varphi)$, the probabilities P_{ie} are unaffected when adding or subtracting terms proportional to unity to the Hamiltonian. We define a new Hamiltonian as

$$H_{\text{new}} = H_{\text{old}} - \frac{1}{2}\text{tr}\,(H_{\text{old}}) \cdot \mathbf{1}, \tag{4.19}$$

where $\mathbf{1}$ is the 2×2 identity matrix. The new Hamiltonian in the mass eigenstate basis is now

$$H_m = \frac{1}{2} \begin{pmatrix} -K + V_E\cos(2\theta) & V_E\sin(2\theta) \\ V_E\sin(2\theta) & K - V_E\cos(2\theta) \end{pmatrix}, \tag{4.20}$$

where $K = \frac{\Delta m^2}{2p} \simeq \frac{\Delta m^2}{2E}$. This Hamiltonian can be written in terms of the Pauli matrices as

$$H_m = \frac{1}{2}\left[V_E\sin(2\theta)\sigma_1 + (V_E\cos(2\theta) - K)\sigma_3\right]. \tag{4.21}$$

As a result of the Hamiltonian being constant in time, the solution to the differential equation (4.5) is

$$|\nu_i(t)\rangle = \mathcal{T}(t)\,|\nu_i\rangle\,, \tag{4.22}$$

where the time evolution operator $\mathcal{T}(t)$ is given by

$$\mathcal{T}(t) = \exp(-\mathrm{i}Ht). \tag{4.23}$$

Since $(\boldsymbol{b}\cdot\boldsymbol{\sigma})^2 = \boldsymbol{b}^2$ is true for any vector $\boldsymbol{b}\in\mathbb{R}^3$, it also holds that

$$\exp\left(-\mathrm{i}k\boldsymbol{b}\cdot\boldsymbol{\sigma}\right) = \mathbf{1}\cos(kb) - \mathrm{i}\frac{\boldsymbol{b}\cdot\boldsymbol{\sigma}}{b}\sin(kb), \tag{4.24}$$

where $b = |\boldsymbol{b}|$. As we saw in Eq. (4.21), the Hamiltonian in the mass basis can be written as $H_m = \boldsymbol{a}\cdot\boldsymbol{\sigma}$, where

$$\boldsymbol{a} = \frac{1}{2}\begin{pmatrix} V_E\sin(2\theta) \\ 0 \\ V_E\cos(2\theta) - K \end{pmatrix}. \tag{4.25}$$

Thus, from Eq. (4.24) it follows that

$$\mathcal{T}_m(t) = \exp(-\mathrm{i}\boldsymbol{a}\cdot\boldsymbol{\sigma}t) = \mathbf{1}\cos(at) - \mathrm{i}\frac{\boldsymbol{a}\cdot\boldsymbol{\sigma}}{a}\sin(at), \tag{4.26}$$

where

$$a = \frac{1}{2}\sqrt{V_E^2 - 2KV_E\cos(2\theta) + K^2}. \tag{4.27}$$

The ket vectors $|\nu_2\rangle$ and $|\nu_e\rangle$ are expressed in the mass eigenstate basis as

$$|\nu_2\rangle_m = \begin{pmatrix} 0 \\ 1 \end{pmatrix}\,,\ |\nu_e\rangle_m = U^\dagger\begin{pmatrix} 1 \\ 0 \end{pmatrix} = \begin{pmatrix} \cos\theta \\ \sin\theta \end{pmatrix}. \tag{4.28}$$

Now, we may easily calculate the amplitude $A_{2e} = \langle\nu_e|\nu_2(L)\rangle$ by using the explicit form of the Pauli matrices. The result is

$$A_{2e} = \langle\nu_e\,|\mathcal{T}(L)|\,\nu_2\rangle = \sin\theta\left[\cos(aL) - \frac{\mathrm{i}}{2a}(V_E + K)\sin(aL)\right], \tag{4.29}$$

from which we easily find that

$$\begin{aligned} P_{2e} &= |A_{2e}|^2 \\ &= \frac{\sin^2\theta}{4a^2}[K^2 + V_E^2 + 2KV_E(\sin^2\theta - \cos(2aL)\cos^2\theta)] \\ &= \sin^2\theta + \frac{KV_E}{4a^2}\sin^2(2\theta)\sin^2(aL). \end{aligned} \tag{4.30}$$

When $L = 0$ or $V_E = 0$, we obtain $P_{2e} = \sin^2\theta = |U_{e2}|^2$, and thus, $P_{n-d} = 0$ just as expected.

4.2.3 The final expression for P_{n-d}

Finally, we insert the expressions we obtained for P_S and P_{2e} into Eq. (4.11). The result of this is

$$P_{n-d} = -D_{2\nu}\frac{KV_E}{4a^2}\sin^2(2\theta)\sin^2(aL). \tag{4.31}$$

Note that when $K \gg V_E$, which is the case for the MSW solutions of the solar neutrino problem, one has $a \simeq \frac{K}{2}$ and Eq. (4.31) takes on the form

$$P_{n-d} \simeq -2D_{2\nu}\frac{EV_E}{\Delta m^2}\sin^2(2\theta)\sin^2\left(\frac{\Delta m^2}{4E}L\right). \tag{4.32}$$

4.3 The case of three neutrino flavors

So far, every analysis of the day-night effect has, to the author's knowledge, been done in the framework of two neutrino flavors. However, we know that there are (at least) three flavors of neutrinos. The reason for using only two flavors has been that the leptonic mixing angle θ_{13} is known to be small [55, 56] leading to an approximate two flavor case. The main goal of this diploma thesis has been to find the effects on the day-night asymmetry induced by using a non-zero mixing angle θ_{13}.

In order to investigate the day-night effect for the case of three neutrino flavors, we will use an approach which is similar to the one used for the two flavor case above. There are certain difficulties in the three flavor case which are not present in the two flavor case. These will be pointed out when encountered. Throughout this section, we will use the standard parameterization of the 3×3 leptonic mixing matrix U [see Eq. (2.29)].

For three neutrino flavors, Eq. (4.2) becomes

$$\begin{aligned} P_S &= k_1c_{12}^2c_{13}^2 + k_2s_{12}^2c_{13}^2 + k_3s_{13}^2 \\ &= c_{13}^2c_{12}^2 - k_2c_{13}^2\cos(2\theta_{12}) + k_3(s_{13}^2 - c_{13}^2c_{12}^2), \end{aligned} \tag{4.33}$$

where $s_{ij} = \sin\theta_{ij}$, $c_{ij} = \cos\theta_{ij}$ and we have eliminated k_1 by using Eq. (4.3). Here we encounter the first difficulty that was not present in the two flavor case. In the two flavor case, we were able to eliminate all but one of the k_i's by means of Eq. (4.3). This is not possible in the three flavor case. However, even in the two flavor case we actually obtained expressions for all k_i, which means that also in the three flavor case, we will have to calculate all k_i.

As in the two flavor case, we may use unitarity conditions to eliminate k_1 and P_{1e} from the expression for P_S. In the three flavor case, this yields

$$P_{SE} = 2\left(k_2 - \frac{1}{2}\right)\left(P_{2e} - \frac{1}{2}\right) + 2\left(k_3 - \frac{1}{2}\right)\left(P_{3e} - \frac{1}{2}\right) + k_2P_{3e} + k_3P_{2e}. \tag{4.34}$$

Observe that as for P_S, there are two k_i's remaining and in addition, there are two P_{ie}'s remaining as well.

4.3.1 Production and propagation in the Sun

In the three flavor framework, there are a number of issues of the neutrino production and propagation in the Sun, which are not present in the two flavor framework. First of all, the three energy levels of neutrino matter eigenstates in general allow two MSW resonances. The matter dependence of the mixing parameters are far from as simple as in the two flavor case. Thus, we have to make certain approximations.

Repeating the approach made in the two flavor case, we obtain the following expression for k_i

$$k_i = \int_0^{R_\odot} \mathrm{d}r f(r) \sum_{j=1}^{3} |\hat{U}_{ej}|^2 P^s_{ji}. \tag{4.35}$$

As we saw in Chapter 3, the second resonance in the three flavor case occurs at $V_{CC} \simeq \frac{\Delta M^2}{2E}\cos(2\theta_{13})$ assuming that the resonances are fairly separated. The maximal electron number density in the Sun, according to the Standard Solar Model (SSM) [24], is about $N_e \simeq 102\ N_A/\mathrm{cm}^3$, which yields a maximal effective potential of $V_{CC,\max} \simeq 7.8 \cdot 10^{-18}$ MeV. Assuming the large mass squared difference ΔM^2 to be of the order of the atmospheric mass squared difference ($|\Delta m^2_{\mathrm{atm}}| \simeq 2 \cdot 10^{-3}$ eV^2), E to be of the order of 10 MeV, and θ_{13} to be small, we find that $\left|\frac{\Delta M^2}{2E}\right| \cos(2\theta_{13}) \simeq 10^{-16}$ MeV. Thus, the solar neutrinos never pass through the second resonance, regardless of the sign of the large mass squared difference. This can be seen in Fig. 4.2, where the energy of the neutrino energy eigenstates in the Sun and the effective solar potential are plotted.

Since the neutrinos never pass through the second resonance, it is a good approximation to assume that the matter eigenstate $|\nu_{M,3}\rangle$ evolves adiabatically, and thus, we have

$$P^s_{3k} = P^s_{k3} = \delta_{3k}. \tag{4.36}$$

As in the two flavor case, it follows from unitarity that

$$P^s_{12} = P^s_{21} = P_{\mathrm{jump}}. \tag{4.37}$$

Furthermore, we make the assumption that $V_{CC} \lesssim \frac{\Delta m^2}{2E} \ll \frac{\Delta M^2}{2E}$. Thus, the neutrino evolution is well approximated by the energy eigenstate $|\nu_{M,3}\rangle$ evolving as the mass eigenstate $|\nu_3\rangle$ and the remaining neutrino states oscillating according to the two flavor case with the effective potential $V_{\mathrm{eff}} = c^2_{13} V_{CC}$. This does not change the probability P_{jump} as calculated with a linear approximation of the potential in the two flavor case, which means that we may use Eq. (3.30) even if the resonance point, where $\left|\frac{N_e}{N_e}\right|$ is to be evaluated, does change. However, in the Sun, N_e is approximately exponentially decaying with the radius of the Sun leading to $\left|\frac{N_e}{N_e}\right|$ being approximately constant, and thus, independent of the point of evaluation.

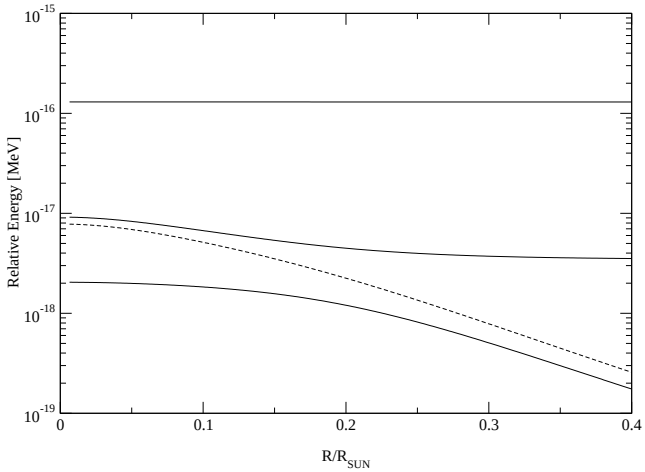

Figure 4.2. The energy of the neutrino energy eigenstates in the Sun relative to the energy of the lowest mass eigenstate energy in vacuum. The dashed curve represents the effective solar potential V_{CC}. The fundamental oscillation parameters are set to the best-fit values of Table 3.2 and the momentum of the neutrinos is $p = 10$ MeV.

To make one further approximation, as long as the effective solar potential is much smaller than the large mass squared difference ΔM^2, the mixing angle $\hat{\theta}_{13} \simeq \theta_{13}$ giving

$$k_3 \simeq \int_0^{R_\odot} \mathrm{d}r f(r) \sin^2\theta_{13} = \sin^2\theta_{13}. \tag{4.38}$$

Regarding the effective solar potential as a perturbation, the absolute first order correction to U_{e3} is

$$U_{e3,\mathrm{corr}} = s_{13}c_{13}^2 \frac{2V_{CC}E}{\Delta m_{31}^2}. \tag{4.39}$$

In addition, the oscillations between the matter eigenstates $|\nu_{M,1}\rangle$ and $|\nu_{M,2}\rangle$ are then well approximated by the two flavor case, using the small mass squared difference Δm^2, the mixing angle θ_{12}, and the effective potential $V_{\mathrm{eff}} = c_{13}^2 V_{CC}$. Thus, we obtain

$$k_1 \simeq c_{13}^2 \frac{1 + D_{3\nu}}{2}\ , \quad k_2 \simeq c_{13}^2 \frac{1 - D_{3\nu}}{2}, \tag{4.40}$$

where

$$D_{3\nu} = \int_0^{R_\odot} \mathrm{d}r f(r) \cos(2\hat{\theta}_{12}(r))(1 - 2P_{\mathrm{jump}}) \tag{4.41}$$

and $\hat{\theta}_{12}(r)$ is calculated in the same way as in the two flavor case using the effective potential. In Fig. 4.3, we can observe how this approximation affects $|U_{ei}|^2$ as a

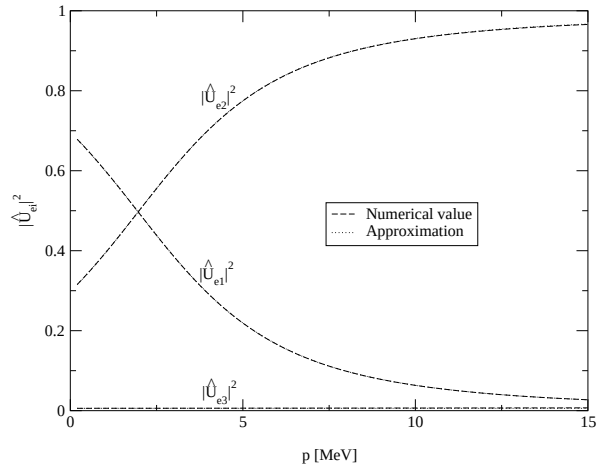

Figure 4.3. The quantity $|\hat{U}_{ei}|^2$ as a function of the neutrino momentum p. This figure shows how the approximation of $\hat{\theta}_{13} \simeq \theta_{13}$ affects $|\hat{U}_{ei}|^2$. Here, V_{CC} is $7.07 \cdot 10^{-18}$ MeV, the value obtained where most of the solar ^{8}B neutrinos are produced and the fundamental neutrino parameters are set to the best-fit values of Table 3.2.

function of the neutrino momentum p. As can be seen in this figure, the approximation is very good for both $|\hat{U}_{e2}|^2$ and $|\hat{U}_{e3}|^2$. For $|\hat{U}_{e1}|^2$, the approximation is even better and the graphs of the approximation and the numerical calculation cannot be distinguished by inspection. Inserting this into Eq. (4.33), we obtain for the three flavor case

$$P_S = s_{13}^4 + c_{13}^4 \frac{1 + D_{3\nu} \cos(2\theta_{12})}{2}. \tag{4.42}$$

When $\theta_{13} \to 0$, we have $D_{3\nu} \to D_{2\nu}$, and thus, we recover the two flavor survival probability.

4.3.2 Propagation in the Earth

As in the case of propagation in the Sun, $V_{CC} \lesssim \frac{\Delta m^2}{2E} \ll \frac{\Delta M^2}{2E}$ and $|\nu_{M,3}\rangle \simeq |\nu_3\rangle$ and the remaining two neutrino eigenstates evolve according to the two flavor case with an effective potential of $V_{\text{eff}} = c_{13}^2 V_{CC}$. For the MSW solutions to the solar neutrino problem together with the assumption that ΔM^2 is of the same order as the atmospheric mass squared difference, this condition is well satisfied for solar neutrinos propagating through the Earth. As a direct result, we obtain the probability P_{3e} as

$$P_{3e} = |\langle \nu_e | \tilde{\nu}_3 \rangle|^2 \simeq |\langle \nu_e | \nu_3 \rangle|^2 = |U_{e3}|^2 = s_{13}^2. \tag{4.43}$$

For the evolution of $|\nu_1\rangle$ and $|\nu_2\rangle$, the approximation yields in the mass eigenstate basis

$$|\nu_i(t)\rangle_m \simeq \begin{pmatrix} |\nu_i(t)\rangle_{m,2\nu} \\ 0 \end{pmatrix}, \quad i \in \{1,2\}, \tag{4.44}$$

where $|\nu_i(t)\rangle_{m,2\nu}$ are the corresponding vectors in the two flavor case with $\theta = \theta_{12}$ and using $c_{13}^2 V_E$ as the effective Earth potential.

In the three flavor case, $|\nu_e\rangle$ is expressed as

$$|\nu_e\rangle_m = U^\dagger \begin{pmatrix} 1 \\ 0 \\ 0 \end{pmatrix} = \begin{pmatrix} c_{13}c_{12} \\ c_{13}s_{12} \\ s_{13} \end{pmatrix} = \begin{pmatrix} c_{13}\,|\nu_e\rangle_{m,2\nu} \\ s_{13} \end{pmatrix} \tag{4.45}$$

in the mass eigenstate basis. Thus, it follows in the three flavor case that

$$\begin{aligned} P_{2e} &= |\,\langle\nu_e|\tilde{\nu}_2\rangle\,|^2 \\ &= c_{13}^2 |\,\langle\nu_e|\tilde{\nu}_2\rangle_{2\nu}\,|^2 \\ &= \frac{c_{13}^2 s_{12}^2}{4a^2}[K^2 + c_{13}^4 V_E^2 + 2c_{13}^2 K V_E(s_{12}^2 - \cos(2aL)c_{12}^2)] \\ &= c_{13}^2 s_{12}^2 + c_{13}^4 \frac{KV_E}{4a^2}\sin^2(2\theta_{12})\sin^2(aL), \end{aligned} \tag{4.46}$$

where the parameter a is calculated using the effective potential $c_{13}^2 V_E$. Again, we observe that when $L = 0$ or $V_E = 0$, we obtain $P_{2e} = c_{13}^2 s_{12}^2 = |U_{e2}|^2$ just as we expect.

4.3.3 The final expression for P_{n-d}

Now we insert the analytical expressions obtained in the previous two sections into Eq. (4.34) and subtract P_S in order to obtain an expression for P_{n-d} in the three flavor framework. After some simplifications, we obtain

$$P_{n-d} = -c_{13}^6 D_{3\nu} \frac{KV_E}{4a^2}\sin^2(2\theta_{12})\sin^2(aL), \tag{4.47}$$

where $K = \frac{\Delta m^2}{2E}$. As in the two flavor case, $K \gg c_{13}^2 V_E$, and thus, $a \simeq \frac{K}{2}$ yielding

$$P_{n-d} \simeq -2c_{13}^6 D_{3\nu} \frac{EV_E}{\Delta m^2}\sin^2(2\theta_{12})\sin^2\left(\frac{\Delta m^2}{4E}L\right). \tag{4.48}$$

Apparently, the effect of using three flavors instead of two is (up to the approximations made) a multiplication by c_{13}^6 as well as a correction in changing $D_{2\nu}$ to $D_{3\nu}$. When $\theta_{13} \to 0$, we have $D_{3\nu} \to D_{2\nu}$, and we clearly obtain the two flavor expression in this limit.

4.4 Incoherent flux approximation

In the discussion above, we have assumed the neutrino flux to be incoherent and we must clearly justify this assumption. This has been done in Ref. [53] for the case of two neutrino flavors. In this section, we summarize this and extend it to the case of three neutrino flavors.

4.4.1 Separation of wave packets

When propagating from the point of production to the point of detection at the Earth, the separation of the mass eigenstate wave packets becomes larger than the size of each individual wave packet. The width σ_x of a wave packet[1] is about $0.9 \cdot 10^{-9}$ m [35] and the coherence length for oscillations including the mass eigenstates $|\nu_i\rangle$ and $|\nu_j\rangle$ is given by

$$L_{\mathrm{coh},ij} = 2\sqrt{2}\frac{2\sigma_x E^2}{|\Delta m^2_{ij}|}. \tag{4.49}$$

The coherence among the mass eigenstates is lost if the traveled length of the neutrinos L is larger than the coherence length $L_{\mathrm{coh},ij}$, i.e., if $L \gg L_{\mathrm{coh},ij}$. We require that all mass eigenstates are incoherent. Since $\Delta m^2_{12} = \Delta m^2 < \Delta m^2_{23} \simeq \Delta m^2_{13} = \Delta M^2$, this holds for all combinations of eigenstates if it holds for the combination $|\nu_1\rangle$ and $|\nu_2\rangle$. From Eq. (4.49) it is also clear that the coherence length increases with energy, which means that if there is incoherence for one energy, there will be incoherence for all lower energies. To include all energies of solar neutrinos, we use $E = 15$ MeV and obtain

$$L_{\mathrm{coh},12} \simeq 1.15 \cdot 10^6 \left(\frac{\mathrm{eV}^2}{\Delta m^2}\right) \text{ m}. \tag{4.50}$$

The distance traveled by the neutrinos is about $L \simeq 1$ AU $\simeq 1.5 \cdot 10^{11}$ m. Hence, the condition $L > L_{\mathrm{coh},12}$ becomes

$$1.15 \cdot 10^6 \left(\frac{\mathrm{eV}^2}{\Delta m^2}\right) \lesssim 1.5 \cdot 10^{11} \quad \Leftrightarrow \quad \Delta m^2 \gtrsim 7.6 \cdot 10^{-6}\ \mathrm{eV}^2, \tag{4.51}$$

which holds for all parts of the LMA solution region.

4.4.2 Eccentricity of the Earth orbit and the Earth diameter

During one year, the distance from the Sun to the Earth changes due to the eccentricity of the Earth orbit. The difference in the Sun-Earth distance is given by $\Delta r = r(\text{aphelion}) - r(\text{perihelion}) = 2e$ AU, where e is the eccentricity of the Earth

[1] This subject is not yet clearly investigated, see Refs. [57–59]. However, we want to estimate the coherence length and use the value of Ref. [35].

orbit with a numerical value of $e \simeq 0.017$. This results in an average change in the distance of $2.83 \cdot 10^7$ m per day. The Earth diameter is approximately $1.3 \cdot 10^7$ m and also gives a daily variation of the same order of magnitude as the eccentricity of the Earth orbit.

The oscillation length induced by the mass eigenstates $|\nu_i\rangle$ and $|\nu_j\rangle$ is given by

$$L_{\mathrm{osc},ij} = \frac{4\pi E}{\Delta m_{ij}^2} \simeq 2.48 \left(\frac{E}{\mathrm{MeV}}\right) \left(\frac{\mathrm{eV}^2}{\Delta m_{ij}^2}\right) \mathrm{m}. \tag{4.52}$$

If the daily change in the distance from the Sun to the Earth is longer than the oscillation length, then any phase dependence will average out during the year. That is, the incoherence assumption will hold as long as $L_{\mathrm{osc},ij} \lesssim 2.83 \cdot 10^7$ m. As in the case of the separation of wave packets, if this condition is satisfied for one energy, then it holds for all energies below that specific energy. We use the energy $E = 15$ MeV to obtain incoherence as a good assumption for all solar neutrinos. The resulting condition is

$$\Delta m_{ij}^2 \geq \Delta m^2 \gtrsim 1.3 \cdot 10^{-6} \mathrm{eV}^2, \tag{4.53}$$

which holds for all MSW solutions to the solar neutrino problem.

4.4.3 Energy resolution of detectors

If we assume that two mass eigenstates (say $|\nu_i\rangle$ and $|\nu_j\rangle$) are in perfect coherence when reaching the Earth, then the relative phase of these eigenstates will be given by

$$\varphi = \frac{\Delta m_{ij}^2 L}{4E}, \tag{4.54}$$

where $L \simeq 1$ AU. The uncertainty in this phase $\delta\varphi$ depends on the uncertainty in the energy δE as

$$\delta\varphi = \left|\frac{\mathrm{d}\varphi}{\mathrm{d}E}\right| \delta E = \frac{\Delta m_{ij}^2 L}{4E^2} \delta E. \tag{4.55}$$

The energy resolution of detectors at solar neutrino energies is approximately given by $\delta E \simeq 0.5 \text{ MeV}\sqrt{(E/\mathrm{MeV})}$. We use the conservative value of $\delta E = 0.1 \text{ MeV}\sqrt{(E/\mathrm{MeV})}$ and obtain

$$\delta\varphi \simeq 4.9 \cdot 10^3 \left(\frac{\Delta m_{ij}^2}{\mathrm{eV}^2}\right) \left(\frac{E}{\mathrm{MeV}}\right)^{-\frac{3}{2}} \left(\frac{L}{\mathrm{m}}\right). \tag{4.56}$$

If $\delta\varphi > 2\pi$, then there will be an effective averaging in the detector, which again justifies the assumption of incoherence. We again use the energy $E = 15$ MeV and obtain the condition

$$\Delta m_{ij}^2 \geq \Delta m^2 \gtrsim 1.9 \cdot 10^{-8} \text{ eV}^2. \tag{4.57}$$

4.5 The day-night effect at detectors

The calculations in the previous part of this chapter give us the day-night asymmetry of the electron neutrino flux at the neutrino energy E as

$$A_{n-d}^{\phi_e}(E) = 2\frac{\phi_{e,N}(E) - \phi_{e,D}(E)}{\phi_{e,N}(E) + \phi_{e,D}(E)} = \frac{P_{n-d}(E)}{P_S(E) + \frac{P_{n-d}(E)}{2}}. \tag{4.58}$$

However, this is *not* the event asymmetry measured at detectors. We will assume a water-Cherenkov detector in which neutrinos are detected by one of the following reactions

$$\nu_x + e^- \longrightarrow \nu_x + e^-, \tag{4.59}$$
$$\nu_x + d \longrightarrow p + p + e^-, \tag{4.60}$$

where $x = e, \mu, \tau$, which are referred to as elastic scattering (ES) and charged-current (CC), respectively. The CC reaction can only occur for $x = e$, since inserting $x \neq e$ in Eq. (4.60) would violate the lepton numbers L_e and L_x. We assume that the scattered electron energy is measured and that the cross-sections $\frac{\mathrm{d}\sigma_{\nu_\mu}}{\mathrm{d}T'}$ and $\frac{\mathrm{d}\sigma_{\nu_\tau}}{\mathrm{d}T'}$ are equal, where T' is the scattered electron energy.

If we denote the zenith angle, i.e., the angle between zenith and the Sun at the detector, by α, then the event rate of measured electrons with energy T in the detector is proportional to

$$R(\alpha, T) = \int_0^\infty \mathrm{d}E\phi(E) \int_0^{T'_{\max}} \mathrm{d}T' F(T, T') \frac{\mathrm{d}\sigma_{\nu_{\text{solar}}}}{\mathrm{d}T'}(T', E, \alpha), \tag{4.61}$$

where $\phi(E)$ is the total solar neutrino flux (see Fig. 3.3), T' is the true electron energy, and $\frac{\mathrm{d}\sigma_{\nu_{\text{solar}}}}{\mathrm{d}T'}$ is given by

$$\frac{\mathrm{d}\sigma_{\nu_{\text{solar}}}}{\mathrm{d}T'} = P_{SE}\frac{\mathrm{d}\sigma_{\nu_e}}{\mathrm{d}T'} + (1 - P_{SE})\frac{\mathrm{d}\sigma_{\nu_\mu}}{\mathrm{d}T'}. \tag{4.62}$$

Here, we have used the assumption $\frac{\mathrm{d}\sigma_{\nu_\mu}}{\mathrm{d}T'} = \frac{\mathrm{d}\sigma_{\nu_\tau}}{\mathrm{d}T'}$, since neutrinos not found in the state $|\nu_e\rangle$ are assumed to be in the state $|\nu_\mu\rangle$ or in the state $|\nu_\tau\rangle$. The energy resolution of the detector is introduced through $F(T, T')$, which is given by

$$F(T, T') = \frac{1}{\Delta_{T'}\sqrt{2\pi}} \exp\left(-\frac{(T - T')^2}{2\Delta_{T'}^2}\right), \tag{4.63}$$

where $\Delta_{T'}$ is the energy resolution at the electron energy T'.

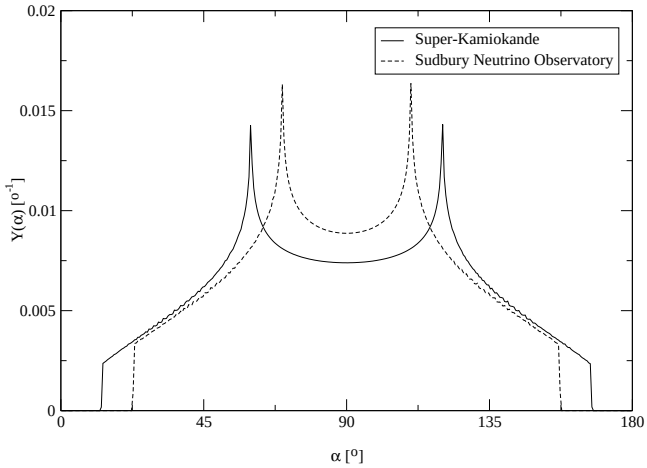

Figure 4.4. The zenith angle exposure function $Y(\alpha)$ for SK and SNO as a function of the zenith angle α. The data are retrieved from Ref. [45].

The night and day rates N and D at the measured electron energy T are given by

$$D(T) = \int_0^{\frac{\pi}{2}} \mathrm{d}\alpha R(\alpha, T) Y(\alpha), \tag{4.64}$$

and

$$N(T) = \int_{\frac{\pi}{2}}^{\pi} \mathrm{d}\alpha R(\alpha, T) Y(\alpha), \tag{4.65}$$

respectively. Here, $Y(\alpha)$ is the zenith angle exposure function, which gives the distribution of exposure time for the different zenith angles. The exposure function is clearly symmetric around $\alpha = \frac{\pi}{2}$ and is plotted in Fig. 4.4 for both SK and SNO. From the night and day rates at a specific electron energy, we define the day-night asymmetry at that energy as

$$A_{n-d}(T) = 2\frac{N(T) - D(T)}{N(T) + D(T)}. \tag{4.66}$$

The final day-night asymmetry is given by integrating the day and night rates over all energies above the detector threshold energy T_{thl}, i.e.,

$$A_{n-d} = 2\frac{\int_{T_{\mathrm{thl}}}^{\infty} \mathrm{d}T(N(T) - D(T))}{\int_{T_{\mathrm{thl}}}^{\infty} \mathrm{d}T(N(T) + D(T))} = 2\frac{N - D}{N + D}. \tag{4.67}$$

The threshold energy T_{thl} is 5 MeV for both SK and SNO.

For computational reasons, we will start by performing the integral over the zenith angle α. For the daytime flux D, $P_{SE} = P_S$, which is independent of α. As a result, the only α dependence is in $Y(\alpha)$ and the zenith angle integral only contributes with a factor one-half (if the normalization of Y is such that $\int_0^\pi \mathrm{d}\alpha Y(\alpha) = 1$). In order to be able to use the results we have obtained for P_{n-d}, we need to compute the difference between the night and day fluxes. This difference is given by

$$N(T) - D(T) = \int_{\frac{\pi}{2}}^{\pi} \mathrm{d}\alpha Y(\alpha) \left[R(\alpha, T) - R(\pi - \alpha, T)\right], \tag{4.68}$$

where we observe that the quantity $R(\alpha, T) - R(\pi - \alpha, T)$ is of the form

$$R(\alpha, T) - R(\pi - \alpha, T) = \int_0^\infty \mathrm{d}E\phi(E) \int_0^{T'_{\max}} \mathrm{d}T' F(T, T') \frac{\mathrm{d}\sigma^{n-d}_{\nu_{\mathrm{solar}}}}{\mathrm{d}T'} \tag{4.69}$$

and

$$\frac{\mathrm{d}\sigma^{n-d}_{\nu_{\mathrm{solar}}}}{\mathrm{d}T'} = P_{n-d}(\alpha, E) \left(\frac{\mathrm{d}\sigma_{\nu_e}}{\mathrm{d}T'} - \frac{\mathrm{d}\sigma_{\nu_\mu}}{\mathrm{d}T'} \right). \tag{4.70}$$

The α dependence in P_{n-d} enters through the length traveled by the neutrinos in the Earth and that the argument aL of the second $\sin^2$-factor in Eq. (4.47) oscillates very fast, and thus, performs an effective averaging of P_{n-d} in the zenith angle integral, i.e., replacing $\sin^2(aL)$ by $\frac{1}{2}$. After this averaging, the only zenith angle dependence left is that of $Y(\alpha)$ and the zenith angle integral only gives us a factor of one-half as in the case of the day rate D.

To avoid having to calculate the night rate N explicitly, we use the simple fact that

$$N = D + (N - D) \tag{4.71}$$

and calculate the day-night asymmetry as

$$A_{n-d} = \frac{N - D}{D + \frac{N-D}{2}}. \tag{4.72}$$

4.5.1 Elastic scattering detection

Neutrinos are detected through ES at both SK and SNO. The ES cross-section in the laboratory frame is given by [40]

$$\frac{\mathrm{d}\sigma_{\nu_\mu}}{\mathrm{d}T'} = \frac{G_F^2 m_e}{2\pi} \left[(g_V^{\nu e} + g_A^{\nu e})^2 + (g_V^{\nu e} - g_A^{\nu e})^2 (1 - y)^2 - (g_V^{\nu e 2} - g_A^{\nu e 2}) \frac{y m_e}{E} \right], \tag{4.73}$$

where G_F is the Fermi coupling constant, m_e the electron mass, E the neutrino energy, $g_X^{\nu e}$ $(X = V, A)$ the vector and axial vector coupling constants, and $y = \frac{T'}{E}$. The cross-section $\frac{\mathrm{d}\sigma_{\nu_e}}{\mathrm{d}T'}$ also involves a Feynman diagram with the exchange of a

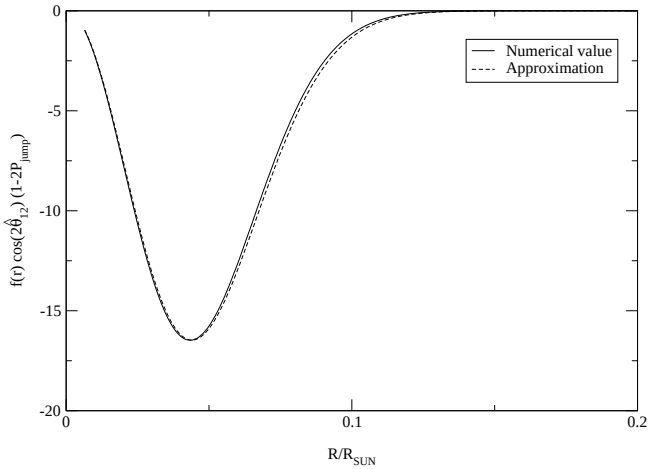

Figure 4.5. The effect of the approximation $V_{CC}(\text{prod.}) = \text{const.} = 7.07 \cdot 10^{-18}$ MeV on the integrand in Eq. (4.41). The best-fit values of Table 3.2 have been used for the fundamental neutrino parameters and the neutrino energy is set to 10 MeV.

W boson and is therefore given by the same expression as in Eq. (4.73) with the substitution $g_X^{\nu e} \to g_X^{\nu e} + 1$. For kinematical reasons, the maximal kinetic energy of the scattered electron in the laboratory frame is given by

$$T'_{\max} = \frac{E}{1 + \frac{m_e}{2E}}. \tag{4.74}$$

The remaining integrals cannot be calculated analytically. Hence, we use numerical methods to evaluate these integrals. However, computing all integrals by numerical methods demands a lot of computer time, and therefore, we make one further approximation, that all solar ^{8}B neutrinos are produced at the solar effective potential is $V_{CC} \simeq 7.07 \cdot 10^{-18}$ MeV, which is the effective potential at the radius where most solar neutrinos are produced. The effect of this approximation on the integrand in Eq. (4.41) is shown in Fig. 4.5.

For the energy resolution of SK, we use [53]

$$\Delta_{T'} = 1.6 \text{ MeV} \sqrt{T'/(10 \text{ MeV})}, \tag{4.75}$$

and for the electron number density in the Earth, we use $N_e = 1.4\ N_A/\text{cm}^3$, where N_A is the Avogadro number, which roughly corresponds to 2.8 g/cm^3 (using $Z/A \simeq 0.5$, where Z is the number of protons and A the number of nucleons for the mantle of the Earth). The electron number density used corresponds to the

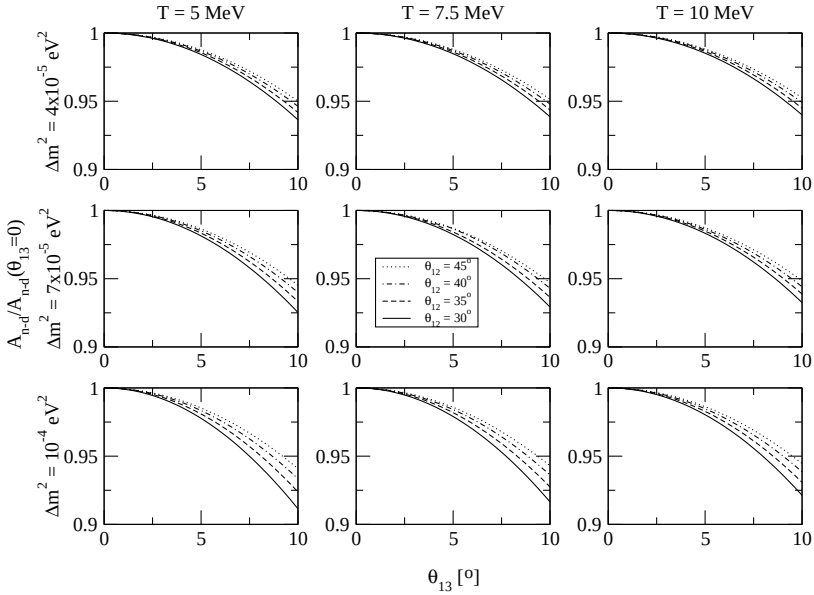

Figure 4.6. The day-night asymmetry at SK for different values of T, Δm^2, and θ_{12} as a function of θ_{13} relative to the corresponding value for $\theta_{13} = 0$.

electron number density in the Earth's crust. This value was used, since the main non-adiabatic density change occurs when the neutrinos enter the Earth. Assuming the rest of the neutrino propagation to be sufficiently adiabatic, only the value of the effective matter potential at entry into the Earth and at detection will play a significant role. In both cases, this is the effective matter potential in the Earth's crust. Note that the regenerative terms in Eqs. (4.32) and (4.48), and thus, the day-night asymmetry, are linearly dependent on the matter potential V_E. It follows that the electron number density used has a great impact on the final results. If we had used the average mantle matter density of about 5 g/cm^3, the resulting asymmetry would increase by almost a factor of two.

The above values give us the numerical results presented in Fig. 4.6. As can be seen from this figure, the relative effect of a non-zero θ_{13} is increasing if the small mass squared difference Δm^2 increases or if the measured electron energy or the leptonic mixing angle θ_{12} decreases. The effect of changing θ_{12} is also clearly larger for smaller electron energy T and larger small mass squared difference Δm^2. In Fig. 4.7, the isocontours of constant day-night asymmetry in the SK detector with θ_{13} equal to 0 and 9.2° are shown for a parameter space covering the LMA solution of the solar neutrino problem. As can be seen from this figure, the variation in

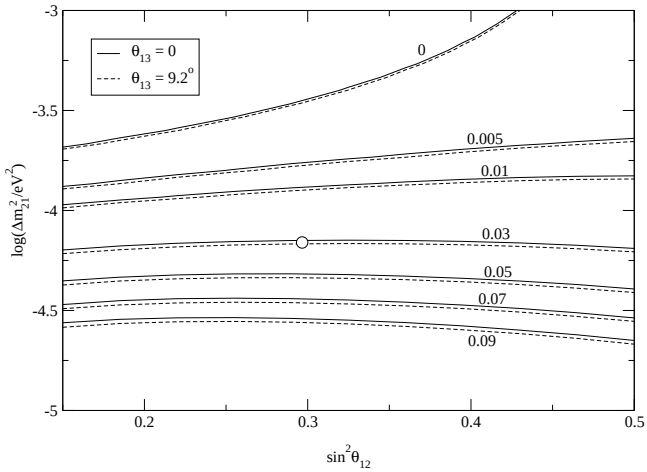

Figure 4.7. Isocontours for the ES day-night asymmetry for two different values of θ_{13}. The values of A_{n-d} for the different isocontours are shown in the figure. The circle corresponds to the best-fit values of Ref. [51].

the isocontours are small compared to the size of the LMA solution and to the current uncertainty in the day-night asymmetry [30, 33]. However, if the values of the parameters θ_{12}, Δm^2, and A_{n-d} were known with a larger accuracy, then the change due to non-zero θ_{13} could, in principle, be used to determine the "reactor" mixing angle θ_{13} as an alternative to long baseline experiments such as neutrino factories [60–62] and super-beams [60, 63–65] as well as future reactor experiments [63] and matter effects for supernova neutrinos [66]. As can be seen from Fig. 4.7, the isocontours are almost horizontal near the best-fit value. Thus, a determination of θ_{13} from the day-night asymmetry is more dependent on the uncertainty in the mass squared difference Δm^2_{21} than the uncertainty in θ_{12}. For the determination to be feasible, the uncertainty in the allowed LMA region as well as the uncertainty in the day-night asymmetry must be smaller than the shift of the isocontours due to a non-zero θ_{13}. This would demand that the uncertainty in Δm^2_{21} must not be larger than a few percent. The day-night asymmetry for the best-fit value of Ref. [51] is $A_{n-d} \simeq 3.0\%$, which is larger than the theoretical value of the SK experiment [30], but still clearly within one standard deviation of the experimental best-fit value.

4.5.2 Charged-current detection

Only SNO uses heavy water, and thus, SNO is the only experimental facility detecting solar neutrinos through the CC reaction (4.60). Since the electron mass m_e

is much smaller than the proton mass m_p ($m_e \simeq 511$ keV, $m_p \simeq 938.3$ MeV), most of the kinetic energy in the center-of-mass frame, which is well approximated by the laboratory frame, since the deuteron mass by far exceeds the neutrino momentum, after the CC reaction will be carried away by the electron. This energy is given by

$$T' = E + \Delta E_{\text{mass}}, \tag{4.76}$$

where $\Delta E_{\text{mass}} = m_d - 2m_p \simeq -1.44$ MeV. Thus, we approximate the differential cross-section $\frac{\mathrm{d}\sigma_{\nu_e}}{\mathrm{d}T'}$ by

$$\frac{\mathrm{d}\sigma_{\nu_e}}{\mathrm{d}T'} = \sigma_{\nu_e}\delta(T' - E + 1.44 \text{ MeV}). \tag{4.77}$$

In the above expression, we use the numerical results given in Ref. [67] and use linear interpolation to calculate the total cross-section σ_{ν_e} as a function of the neutrino energy E. For $x \neq e$, the reaction in Eq. (4.60) is forbidden, since it violates the lepton numbers L_e and L_x. Thus, for $x \neq e$ we have $\frac{\mathrm{d}\sigma_{\nu_x}}{\mathrm{d}T'} = 0$.

The energy resolution at SNO is given by [32, 68]

$$\Delta_{T'} = -0.0684 \text{ MeV} + 0.331 \text{ MeV}\sqrt{\left(\frac{T'}{\text{MeV}}\right)} + 0.0425\text{MeV}\left(\frac{T'}{\text{MeV}}\right). \tag{4.78}$$

This gives the results presented in Fig. 4.8. This figure shows the same main features as Fig. 4.6. However, the effects of different T and Δm^2 are larger in the CC case.

In Fig 4.9, we have plotted isocontours for the CC day-night asymmetry for θ_{13} equal to 0 and 9.2° in order to observe the effect of non-zero θ_{13} for the day-night asymmetry isocontours in the region of the LMA solution. Just as in the case of ES, the isocontours do not change dramatically and the change is small compared to the uncertainty in the day-night asymmetry. It is also apparent that the day-night asymmetry is smaller for the ES detection than for the CC detection. This was to be expected, since the ES detection is sensitive to the fluxes of ν_μ and ν_τ as well as to the ν_e flux, while the CC detection is only sensitive to the ν_e flux. The day-night asymmetry for the best-fit values of Ref. [51] is $A_{n-d} \simeq 4.6\%$, which corresponds rather well to the values presented in Refs. [69, 70].

4.5.3 Neutral-current detection

At SNO, solar neutrinos are also detected through the neutral-current (NC) reaction

$$\nu_x + d \longrightarrow \nu_x + n + p, \tag{4.79}$$

where $x = e, \mu, \tau$. To leading order in the weak coupling constant, the mass of the charged lepton of the same generation as ν_x does not appear in the cross-section. It follows that the cross-section σ_x^{NC} is, to leading order, independent of the lepton generation x and that there will be no day-night effect for neutral-currents. Should such an asymmetry be measured at a high confidence level, then alternative methods of description such as oscillations into sterile neutrinos would be needed.

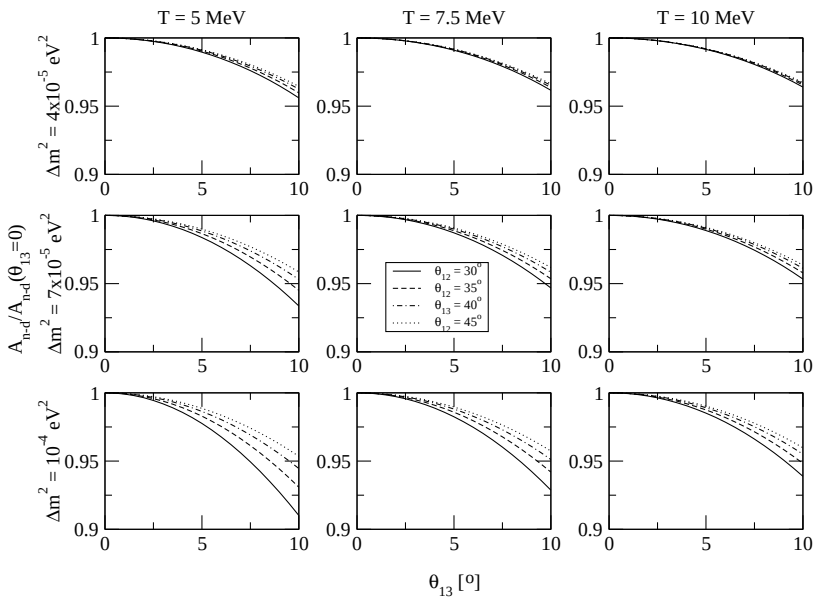

Figure 4.8. The CC day-night asymmetry at SNO for different values of T, Δm^2, and θ_{12} as a function of θ_{13} relative to the corresponding value for $\theta_{13} = 0$.

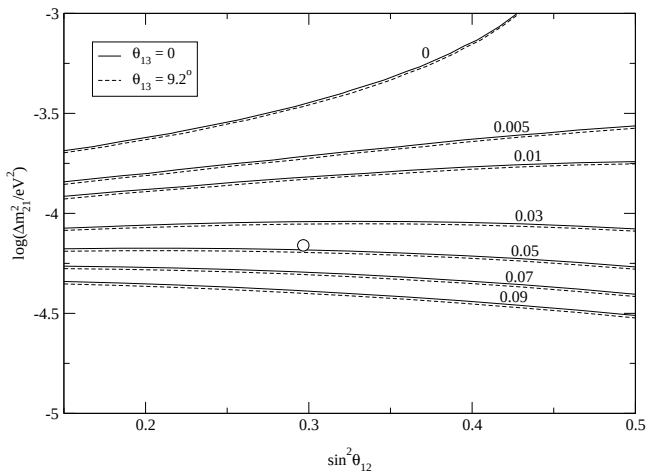

Figure 4.9. Isocontours for the CC day-night asymmetry for two different values of θ_{13}. The values of A_{n-d} for the different isocontours are shown in the figure. The circle corresponds to the best-fit values of Ref. [51].

Chapter 5

Discussion

In this thesis, the day-night effect on the solar electron neutrino flux has been studied in the framework of three neutrino flavors. We have derived analytical expressions for the day P_S and night P_{SE} solar electron neutrino survival probabilities in the case of two and three neutrino flavors. We have used these to numerically compute the day-night asymmetry A_{n-d} for the elastic scattering detection of neutrinos at the Super-Kamiokande experiment and the charged-current detection of neutrinos at the Sudbury Neutrino Observatory.

The final expressions for the regenerative term P_{n-d} in the night survival probability in the two and three flavor frameworks have been obtained as

$$P_{n-d} = -D_{2\nu}\frac{KV_E}{4a^2}\sin^2(2\theta)\sin^2(aL) \tag{5.1}$$

and

$$P_{n-d} = -c_{13}^6 D_{3\nu}\frac{KV_E}{4a^2}\sin^2(2\theta_{12})\sin^2(aL), \tag{5.2}$$

respectively, where $a \simeq \frac{1}{2}K = \frac{\Delta m_{21}^2}{4E} = \frac{\Delta m^2}{4E}$ for the MSW solutions of the solar neutrino problem. The expressions for the regenerative term in the two and three flavor frameworks differ by the substitution of $D_{2\nu} \to D_{3\nu}$ and the introduction of the factor $\cos^6\theta_{13}$ in the three flavor case. An important observation is that we recover the two flavor expression for the regenerative term as $\theta_{13} \to 0$. The result of the above is a small suppression of the regenerative term for non-zero θ_{13} as compared to the two flavor regenerative term.

It should be noted that the expressions for the regenerative terms are linearly dependent on the Earth matter potential V_E for the LMA solution of the solar neutrino problem. Thus, it follows that it is important to carefully choose which value of the potential to use.

In the study of the day-night asymmetry at detectors, it is apparent that the relative effect of non-zero θ_{13} in the LMA region is increasing for increasing Δm^2 as well as for decreasing θ_{12} and decreasing measured electron energy T. The

dependence on θ_{12} is also larger for smaller T and larger Δm^2. This result holds for both the elastic scattering and charged-current detection of neutrinos.

We have also shown that the effects of a non-zero θ_{13} on the isocontours of constant day-night asymmetry A_{n-d} at detectors are small compared to the current experimental uncertainty in A_{n-d}. However, should this uncertainty and the uncertainties in the fundamental parameters θ_{12} and Δm^2_{21} become much smaller in the future, the day-night asymmetry could be used to determine θ_{13} as an alternative to long baseline and future reactor experiments.

Bibliography

[1] J. Chadwick, *The Existence of a Neutron*, Proc. Roy. Soc. A **136**, 692 (1932).

[2] F. Perrin, *Possibilité d'émission de Particules Neutres de Masse Intrinsèque Nulle dans les Radioactivités β*, Comptes Rendues **197**, 1625 (1933).

[3] E. Fermi, *Tentativo di Una Teoria dei Raggi β*, Nuovo Cimento **11**, 1 (1934).

[4] E. Fermi, *Versuch Einer Theorie der β-Strahlen. I.*, Z. Phys. **88**, 161 (1934).

[5] H. Bethe and R. Peierls, *The "Neutrino"*, Nature **133**, 532 (1934).

[6] C. Cowan *et al.*, *Detection of the Free Neutrino: A Confirmation*, Science **124**, 103 (1956).

[7] F. Reines and C. Cowan, *The Neutrino*, Nature **178**, 492 (1956).

[8] B. Pontecorvo, *Mesonium and Antimesonium*, Sov. Phys. JETP **6**, 172 (1958).

[9] B. Pontecorvo, *Inverse Beta Processes and Nonconservation of Lepton Charge*, Sov. Phys. JETP **7**, 172 (1958).

[10] Z. Maki, M. Nakagawa and S. Sakata, *Remarks in the Unified Model of Elementary Particles*, Prog. Theor. Phys. **28**, 870 (1962).

[11] M. Nakagawa *et al.*, *Possible Existence of a Neutrino with Mass and Partial Conservation of Muon Charge*, Prog. Theor. Phys **30**, 727 (1963).

[12] V. Gribov and B. Pontecorvo, *Neutrino Astronomy and Lepton Charge*, Phys. Lett. B. **28**, 493 (1969).

[13] S. M. Bilenky, *Neutrino Oscillations and Neutrino Mixing*, Sov. J. Part. Nucl. **18**, 188 (1987).

[14] S. L. Glashow, *Partial-Symmetries of Weak Interactions*, Nucl. Phys. **22**, 579 (1961).

[15] S. Weinberg, *A Model of Leptons*, Phys. Rev. Lett. **19**, 1264 (1967).

[16] A. Salam, Proceedings of the Eighth Nobel Symposium, edited by N. Svartholm, p. 367, Almqvist och Wiksell, Stockholm, 1968.

[17] M. Gell-Mann, *The Interpretation of the New Particles as Displaced Charged Multiplets*, Nuovo Cimento Suppl. **4**, 848 (1956).

[18] K. Nishijima, *Charge Independence Theory of V Particles*, Prog. Theor. Phys. **13**, 285 (1955).

[19] F. Englert and R. Brout, *Broken Symmetry and the Mass of Gauge Vector Mesons*, Phys. Rev. Lett. **13**, 321 (1964).

[20] P. W. Higgs, *Broken Symmetries, Massless Particles and Gague Fields*, Phys. Lett. **12**, 132 (1964).

[21] G. S. Guralnik, C. R. Hagen and T. W. B. Kibble, *Global Conservation Laws and Massless Particles*, Phys. Rev. Lett. **13**, 585 (1964).

[22] P. W. Higgs, *Spontaneous Symmetry Breakdown without Massless Bosons*, Phys. Rev. **145**, 1156 (1966).

[23] M. C. Gonzalez-Garcia and Y. Nir, *Developments in Neutrino Physics*, Rev. Mod. Phys. **75**, 345 (2003), `hep-ph/0202058`.

[24] J. N. Bahcall, M. H. Pinsonneault and S. Basu, *Solar Models: Current Epoch and Time Dependences, Neutrinos, and Helioseismological Properties*, Astrophys. J. **555**, 990 (2001), `astro-ph/0010346`.

[25] Super-Kamiokande Collaboration, Y. Fukuda *et al.*, *Evidence for Oscillation of Atmospheric Neutrinos*, Phys. Rev. Lett. **81**, 1562 (1998), `hep-ex/9807003`.

[26] K2K Collaboration, S. H. Ahn *et al.*, *Detection of Accelerator Produced Neutrinos at a Distance of 250 km*, Phys. Lett. **B511**, 178 (2001), `hep-ex/0103001`.

[27] K2K Collaboration, M. H. Ahn *et al.*, *Indications of Neutrino Oscillation in a 250 km Long-Baseline Experiment*, Phys. Rev. Lett. **90**, 041801 (2003), `hep-ex/0212007`.

[28] Super-Kamiokande Collaboration, S. Fukuda *et al.*, *Solar* ^8B *and hep Neutrino Measurements From 1258 Days of Super-Kamiokande Data*, Phys. Rev. Lett. **86**, 5651 (2001), `hep-ex/0103032`.

[29] Super-Kamiokande Collaboration, S. Fukuda *et al.*, *Determination of Solar Neutrino Oscillation Parameters Using 1496 Days of Super-Kamiokande-I Data*, Phys. Lett. **B539**, 179 (2002), `hep-ex/0205075`.

[30] Super-Kamiokande Collaboration, M. B. Smy *et al.*, *Precise Measurement of the Solar Neutrino Day/Night and Seasonal Variation in Super-Kamiokande-I*, `hep-ex/0309011`.

[31] SNO Collaboration, Q. R. Ahmad *et al.*, *Measurement of the Charged Current Interactions Produced by ^8B Solar Neutrinos at the Sudbury Neutrino Observatory*, Phys. Rev. Lett. **87**, 071301 (2001), `nucl-ex/0106015`.

[32] SNO Collaboration, Q. R. Ahmad *et al.*, *Direct Evidence for Neutrino Flavor Transformation from Neutral-Current Interactions in the Sudbury Neutrino Observatory*, Phys. Rev. Lett. **89**, 011301 (2002), `nucl-ex/0204008`.

[33] SNO Collaboration, Q. R. Ahmad *et al.*, *Measurement of Day and Night Neutrino Energy Spectra at SNO and Constraints on Neutrino Mixing Parameters*, Phys. Rev. Lett. **89**, 011302 (2002), `nucl-ex/0204009`.

[34] SNO Collaboration, S. N. Ahmed *et al.*, *Measurement of the Total Active ^8B Solar Neutrino Flux at the Sudbury Neutrino Observatory With Enhanced Neutral-Current Sensitivity*, `nucl-ex/0309004`.

[35] C. W. Kim and A. Pevsner, *Neutrinos in Physics and Astrophysics*, Chur, Switzerland: Harwood (1993) 429 p. (Contemporary concepts in physics, 8).

[36] Z. Maki, M. Nakagawa and S. Sakata, *Remarks on the Unified Model of Elementary Particles*, Prog. Theor. Phys. **28**, 870 (1962).

[37] N. Cabibbo, *Unitary Symmetry and Leptonic Decays*, Phys. Rev. Lett. **10**, 531 (1963).

[38] M. Kobayashi and T. Maskawa, *CP Violation in the Renormalizable Theory of Weak Interaction*, Prog. Theor. Phys. **49**, 652 (1973).

[39] K. Winter, *Neutrino Physics, 2nd Edition*, Cambridge University Press (2000) 576 p.

[40] Particle Data Group, K. Hagiwara *et al.*, *Review of Particle Physics*, Phys. Rev. **D66**, 010001 (2002).

[41] L. Wolfenstein, *Neutrino Oscillations in Matter*, Phys. Rev. **D17**, 2369 (1978).

[42] S. P. Mikheev and A. Y. Smirnov, *Resonance Enhancement of Oscillations in Matter and Solar Neutrino Spectroscopy*, Sov. J. Nucl. Phys. **42**, 913 (1985).

[43] E. K. Akhmedov, *Neutrino Physics*, `hep-ph/0001264`.

[44] S. P. Mikheev and A. Y. Smirnov, *Resonance Oscillations of Neutrinos in Matter*, Sov. Phys. Usp. **30**, 759 (1987).

[45] Homepage of J.N. Bahcall, http://www.sns.ias.edu/ jnb/.

[46] S. Turck-Chieze and I. Lopes, *Toward a Unified Classical Model of the Sun: On the Sensitivity of Neutrinos and Helioseismology to the Microscopic Physics*, Astrophys. J. **408**, 347 (1993).

[47] Homestake Collaboration, B. T. Cleveland *et al.*, *Measurement of the Solar Electron Neutrino Flux With the Homestake Chlorine Detector*, Astrophys. J. **496**, 505 (1998).

[48] SAGE Collaboration, J. N. Abdurashitov *et al.*, *Measurement of the Solar Neutrino Capture Rate by the Russian-American Gallium Solar Neutrino Experiment During One Half of the 22-year Cycle of Solar Activity*, J. Exp. Theor. Phys. **95**, 181 (2002), `astro-ph/0204245`.

[49] GALLEX Collaboration, W. Hampel *et al.*, *GALLEX Solar Neutrino Observations: Results for GALLEX IV*, Phys. Lett. **B447**, 127 (1999).

[50] KamLAND Collaboration, K. Eguchi *et al.*, *First Results from KamLAND: Evidence for Reactor Anti- Neutrino Disappearance*, Phys. Rev. Lett. **90**, 021802 (2003), `hep-ex/0212021`.

[51] M. Maltoni *et al.*, *Status of Three-Neutrino Oscillations After the SNO-salt Data*, `hep-ph/0309130`.

[52] A. M. Dziewonski and D. L. Anderson, *Preliminary Reference Earth Model*, Phys. Earth Planet. Interiors **25**, 297 (1981).

[53] A. H. Guth, L. Randall and M. Serna, *Day-Night and Energy Variations for Maximal Neutrino Mixing Angles*, JHEP **08**, 018 (1999), `hep-ph/9903464`.

[54] M. Freund and T. Ohlsson, *Matter Enhanced Neutrino Oscillations With a Realistic Earth Density Profile*, Mod. Phys. Lett. **A15**, 867 (2000), `hep-ph/9909501`, and references therein.

[55] CHOOZ Collaboration, M. Apollonio *et al.*, *Limits on Neutrino Oscillations From the CHOOZ Experiment*, Phys. Lett. **B466**, 415 (1999), `hep-ex/9907037`.

[56] CHOOZ Collaboration, M. Apollonio *et al.*, *Search for Neutrino Oscillations on a Long-Baseline at the CHOOZ Nuclear Power Station*, Eur. Phys. J. **C27**, 331 (2003), `hep-ex/0301017`.

[57] C. Giunti and C. W. Kim, *Coherence of Neutrino Oscillations in the Wave Packet Approach*, Phys. Rev. **D58**, 017301 (1998), `hep-ph/9711363`.

[58] W. Grimus, P. Stockinger and S. Mohanty, *The Field-Theoretical Approach to Coherence in Neutrino Oscillations*, Phys. Rev. **D59**, 013011 (1999), `hep-ph/9807442`.

[59] C. Y. Cardall, *Coherence of Neutrino Flavor Mixing in Quantum Field Theory*, Phys. Rev. **D61**, 073006 (2000), `hep-ph/9909332`.

[60] P. Huber, M. Lindner and W. Winter, *Superbeams Versus Neutrino Factories*, Nucl. Phys. **B645**, 3 (2002), `hep-ph/0204352`.

[61] M. Apollonio *et al.*, *Oscillation Physics With a Neutrino Factory*, `hep-ph/0210192`.

[62] Muon Collider/Neutrino Factory Collaboration, M. M. Alsharoa *et al.*, *Recent Progress in Neutrino Factory and Muon Collider Research Within the Muon Collaboration*, Phys. Rev. ST Accel. Beams **6**, 081001 (2003), `hep-ex/0207031`.

[63] P. Huber *et al.*, *Reactor Neutrino Experiments Compared to Superbeams*, Nucl. Phys. **B665**, 487 (2003), `hep-ph/0303232`.

[64] Y. Itow *et al.*, *The JHF-Kamioka Neutrino Project*, `hep-ex/0106019`.

[65] D. Ayres *et al.*, *Letter of Intent to Build an Off-Axis Detector to Study $\nu_\mu \to \nu_e$ Oscillations With the NuMI Neutrino Beam*, `hep-ex/0210005`.

[66] A. S. Dighe, M. T. Keil and G. G. Raffelt, *Identifying Earth Matter Effects on Supernova Neutrinos at a Single Detector*, JCAP **0306**, 006 (2003), `hep-ph/0304150`.

[67] S. Ando *et al.*, *Solar-Neutrino Reactions on Deuteron in Effective Field Theory*, Phys. Lett. **B555**, 49 (2003), `nucl-th/0206001`.

[68] SNO HOWTO kit, http://www.sno.phy.queensu.ca/sno/.

[69] P. C. de Holanda and A. Y. Smirnov, *Solar neutrinos: The SNO Salt Phase Results and Physics of Conversion*, `hep-ph/0309299`.

[70] A. Bandyopadhyay *et al.*, *Constraints on Neutrino Oscillation Parameters From the SNO Salt Phase Data*, `hep-ph/0309174`.